



**HAL**  
open science

# The kinetics of $X + H_2$ reactions ( $X = C(1D), N(2D), O(1D), S(1D)$ ) at low temperature: recent combined experimental and theoretical investigations

Kevin Hickson, Pascal Larrégaray, Laurent Bonnet, Tomás González-Lezana

## ► To cite this version:

Kevin Hickson, Pascal Larrégaray, Laurent Bonnet, Tomás González-Lezana. The kinetics of  $X + H_2$  reactions ( $X = C(1D), N(2D), O(1D), S(1D)$ ) at low temperature: recent combined experimental and theoretical investigations. *International Reviews in Physical Chemistry*, 2021, 40 (4), pp.457-493. 10.1080/0144235X.2021.1976927 . hal-03374348

**HAL Id: hal-03374348**

**<https://hal.science/hal-03374348>**

Submitted on 12 Oct 2021

**HAL** is a multi-disciplinary open access archive for the deposit and dissemination of scientific research documents, whether they are published or not. The documents may come from teaching and research institutions in France or abroad, or from public or private research centers.

L'archive ouverte pluridisciplinaire **HAL**, est destinée au dépôt et à la diffusion de documents scientifiques de niveau recherche, publiés ou non, émanant des établissements d'enseignement et de recherche français ou étrangers, des laboratoires publics ou privés.

## Review

### ***The kinetics of $X + H_2$ reactions ( $X = C(^1D)$ , $N(^2D)$ , $O(^1D)$ , $S(^1D)$ ) at low temperature: Recent combined experimental and theoretical investigations***

Kevin M. Hickson<sup>a,b</sup>, Pascal Larrégaray<sup>a,b</sup>, Laurent Bonnet<sup>a,b</sup> and Tomás González-Lezana<sup>c†</sup>

<sup>a</sup>*Université de Bordeaux, Institut des Sciences Moléculaires, F-33400 Talence, France;*

<sup>b</sup>*CNRS, Institut des Sciences Moléculaires, F-33400 Talence, France;*

<sup>c</sup>*Instituto de Física Fundamental, Consejo Superior de Investigaciones Científicas IFF-CSIC, Serrano 123, 28006 Madrid, Spain*

(June 2021)

In recent years, combined experimental and theoretical efforts have brought valuable information on the kinetics of reactive collisions between molecular hydrogen and an electronically excited atom X (where  $X = C(^1D)$ ,  $N(^2D)$ ,  $O(^1D)$  or  $S(^1D)$ ). These four reactions have been comparatively studied together in numerous occasions in the past due to the similar importance of complex-forming mechanisms found in their overall dynamics. In this work, we compile the most updated information on these investigations making a special emphasis from the theoretical side on statistically based techniques, in an attempt to test the possible insertion nature of the overall dynamics. Besides a description of the experimental details of the kinetics investigation, a comparison of the measured rate constants over a temperature range between 50 K and 300 K with the most recent theoretical calculations is presented.

Contents	PAGE
<b>1. Introduction</b>	2
<b>2. The experiment</b>	2
2.1 Temperature dependent rate constants	8
2.2 Product branching ratios	12
<b>3. Theory for complex-forming reactions</b>	14
3.1 Statistical quantum method	15
3.2 Mean potential phase space theory	16
3.3 Mean potential capture theory	16
3.4 Semiclassical capture theory	16
<b>4. <math>C(^1D) + H_2</math></b>	17
<b>5. <math>N(^2D) + H_2</math></b>	20
<b>6. <math>O(^1D) + H_2</math></b>	24
<b>7. <math>S(^1D) + H_2</math></b>	28
<b>8. Conclusions</b>	32

---

† Email: t.gonzalez.lezana@csic.es

## 9. Acknowledgments

32

### 1. Introduction

Over two decades ago, reactive collisions between molecular hydrogen and an electronically excited atom of either C(<sup>1</sup>D), N(<sup>2</sup>D), O(<sup>1</sup>D) or S(<sup>1</sup>D) were in the agenda of many groups interested in probing their state-to-state dynamics of by means of experimental techniques such as H-atom Rydberg tagging time-of-flight (TOF) spectroscopy [1, 2], or by mapping out the differential cross section (DCS) via Doppler-selected TOF methods in crossed-molecular-beam (CMB) experiments [3–8]. As a prototype of insertion processes, in which the reaction is mediated by the existence of a relatively deep potential well in the intermediate region between reactants and products (with values of the potential depth of  $\sim -4.29$  eV for C(<sup>1</sup>D)+H<sub>2</sub>,  $\sim -5.48$  eV for N(<sup>2</sup>D)+H<sub>2</sub>,  $\sim -7.29$  eV for O(<sup>1</sup>D)+H<sub>2</sub> and  $\sim -4.23$  eV for S(<sup>1</sup>D)+H<sub>2</sub>, respectively), a complex-forming mechanism is assumed to govern their overall dynamics for the ground electronic state. Thus, among the different numerical approaches employed in the corresponding theoretical investigations, approximate statistical and capture theory techniques have proved to be remarkably good alternatives to computationally expensive exact quantum mechanical (QM) methods. This similarity in the overall dynamics is one of the reasons why these four reactions have been treated together on numerous occasions in the past [9–12].

More recently, a series of kinetics investigations have provided valuable information regarding the rate constants at temperatures between 50 and 300 K. In this work, we review the experimental efforts to characterize the reactions outlined above in this low temperature regime, making a special emphasis on the numerical predictions obtained by means of statistically based techniques to test their validity to interpret the measurements. These combined experimental and theoretical studies are completed by comparison with existing information in the literature.

The review is structured as follows: First, the experimental setup is explained in Section 2, indicating the procedure followed to obtain the temperature dependent rate constant and to extract product branching ratios between the two possible exit channels when one of the hydrogen atoms in the H<sub>2</sub> reactant is substituted by deuterium. In Section 3 details of the theoretical approaches under consideration are briefly discussed; in Sections 4 to 7, we present results for the C(<sup>1</sup>D)+H<sub>2</sub>, N(<sup>2</sup>D)+H<sub>2</sub>, O(<sup>1</sup>D)+H<sub>2</sub> and S(<sup>1</sup>D)+H<sub>2</sub> reactions, respectively and finally, conclusions are shown in Section 8, and acknowledgments are given in Section 9.

### 2. The experiment

While experimental studies of the kinetics of gas-phase reactions are relatively straightforward at temperatures greater than 200 K through the application of cryogenic cooling methods, at lower temperatures many gaseous reagents and precursor molecules are difficult to maintain in the gas-phase due to their low saturated vapour pressures. As the temperature falls below 100 K, these molecules begin to condense on the walls of the reaction vessel, limiting the use of cryogenic based methods to study

reactivity at temperatures pertinent to interstellar environments. Although molecular hydrogen and its isotopologues HD and D<sub>2</sub> remain in the gas-phase to temperatures well below 20 K, all of the precursor molecules used to create the radical reagent species X (where X = C(<sup>1</sup>D), N(<sup>2</sup>D), O(<sup>1</sup>D) and S(<sup>1</sup>D)) used in this work condense readily at low temperature, precluding the use of this type of reactor to study the kinetics of X + H<sub>2</sub> reactions at low temperatures. In this instance, extensive cooling can be brought about through the use of supersonic expansions such as free jets and Laval nozzle (LN) flows where a high pressure gas is expanded into a low pressure region. Free jet expansions, based on an isentropic expansion of gas molecules to attain low temperatures have been employed in the past by Smith *et al.* [13] to study gas-phase ion-molecule reactions below 20 K. Nevertheless, as the gas continues to expand after exiting the nozzle, the changing density strongly modifies the collision rate making this method less suitable for studying the kinetics of gas-phase reactions. In contrast, the LN technique or CRESU method (Cinétique de Réaction en Écoulement Supersonique Uniforme or Reaction Kinetics in a Uniform Supersonic Flow) employs a specially shaped convergent-divergent nozzle to produce a downstream gas flow with a constant Mach number such that the density and temperature remain constant as a function of distance from the nozzle exit. See Fig. 1 for a schematic representation.

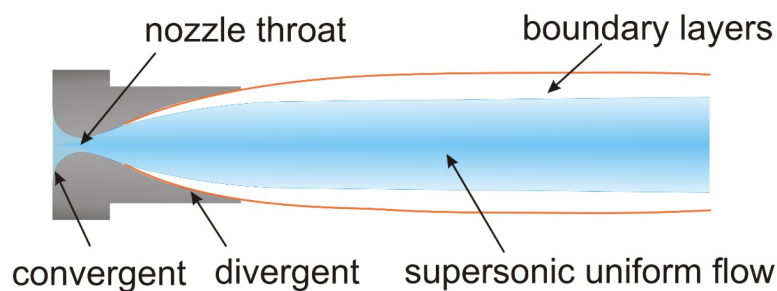


Figure 1. Schematic representation of the Laval nozzle flow.

LN expansions can persist for several tens of centimetres (corresponding to several hundreds of microseconds) thereby representing an important technique to study the kinetics of fast gas-phase reactions at low temperatures. This method was first employed to study ion-molecule reactions in the 1980's [14] before being adapted to investigate reactions between neutral species in the early 1990's [15]. To date, most experimental kinetic studies of gas-phase reactions to have been performed below 100 K have employed the CRESU method. Several excellent review articles of the CRESU method and its application in the field of low temperature chemical kinetics exist (see Potapov *et al.* [16] for example) in the literature. In common with this earlier work, the method of choice to study the kinetics of X + H<sub>2</sub> reactions down to low temperatures is through the application of the CRESU method. The majority of the experimental results described here have been obtained using the Bordeaux CRESU apparatus (the kinetic study of the S(<sup>1</sup>D) + H<sub>2</sub> reaction [17] was performed

on one of the CRESU apparatuses located in the Institut de Physique de Rennes). The Bordeaux system, as shown schematically in Figure 2 for the particular case of  $C(^1D)+H_2$ , is designed around a series of home-built axisymmetric LN.

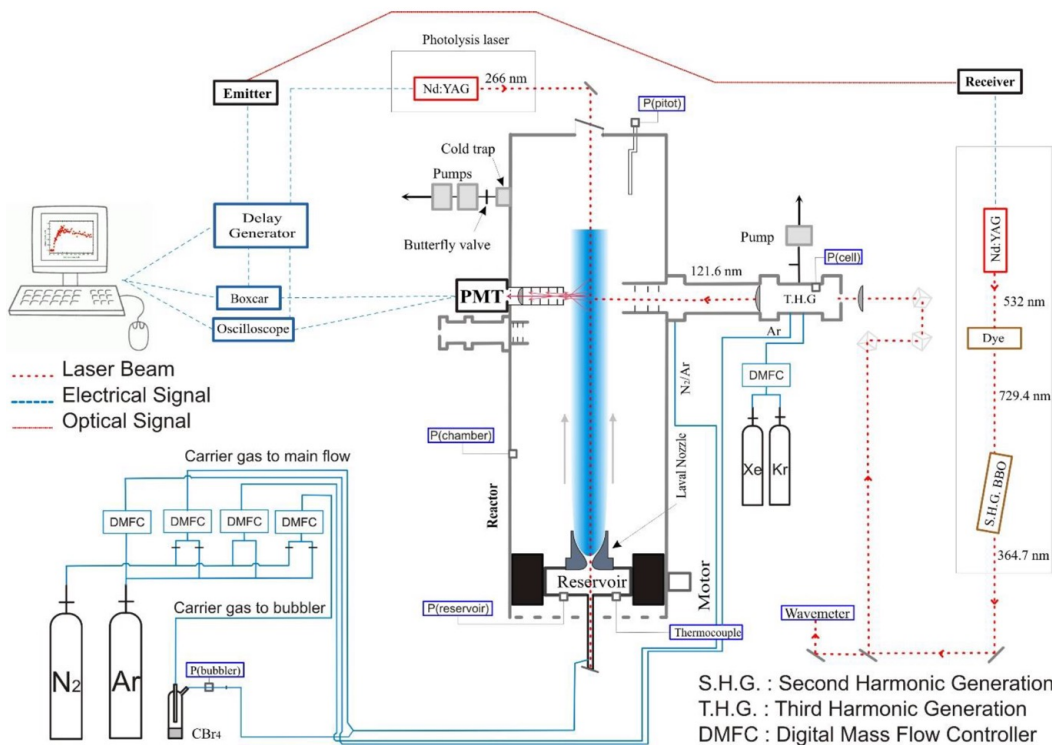


Figure 2. Schematic representation of the CRESU apparatus used to follow  $H(^2S)$  atoms at 121.567 nm, formed by the  $C(^1D) + H_2$  reaction.

The nozzle is attached to the central axis of a cylindrical piston which slides along the inside of a stainless steel reactor, thereby allowing the nozzle-observation axis distance to be varied. Each nozzle is designed to operate with a specified carrier gas under well-defined conditions of upstream pressure (the reservoir or stagnation pressure) and impact pressure (the flow pressure, recorded using a Pitot tube inserted into the cold flow) as measured by capacitance manometers. These optimal operating conditions for each nozzle are chosen to yield minimal variations of the impact pressure as a function of distance from the nozzle, in addition to allowing the cold flow to propagate as far as possible within the chamber. In this way, the flow density and flow temperature are both well defined and constant at all positions within the supersonic flow, while the time available for measurements to be performed is maximized; a critical consideration in particular for “slow reactions” such as  $N(^2D) + H_2$  and  $D_2$ . The relevant characteristics of the Bordeaux Laval nozzles used in this work are provided in Table 1.

In addition to the low temperature studies, measurements were also conducted at room temperature. During these experiments, the LN was removed from the chamber

Table 1. Supersonic flow characteristics.

Mach number	$1.83 \pm 0.02$	$1.99 \pm 0.03$	$2.97 \pm 0.06$	$3.85 \pm 0.05$
Carrier gas	N <sub>2</sub>	Ar	Ar	Ar
Density ( $\times 10^{16}$ cm <sup>-3</sup> )	$9.4 \pm 0.2$	$12.6 \pm 0.3$	$14.7 \pm 0.6$	$25.9 \pm 0.9$
Impact pressure (Torr)	$8.2 \pm 0.1$	$10.5 \pm 0.2$	$15.3 \pm 0.5$	$29.6 \pm 1.0$
Stagnation pressure (Torr)	10.3	13.9	34.9	113
Temperature (K)	$177 \pm 2$	$127 \pm 2$	$75 \pm 2$	$50 \pm 1$
Mean flow velocity (ms <sup>-1</sup> )	$496 \pm 4$	$419 \pm 3$	$479 \pm 3$	$505 \pm 1$
Chamber pressure (Torr)	1.4	1.5	1.2	1.4

while the pressure was maintained around 5 Torr with a total gas-flow of around 6.5 standard litres per minute. Under these conditions, the flow velocity was fast enough to replenish the photolyzed gas between laser shots but it was slow enough to avoid pressure gradients within the reactor. The reaction chamber itself is pumped by a Roots blower backed by a mechanical pump, providing a pumping capacity of 1000 m<sup>3</sup>/hr, which can be varied through the use of a motorized butterfly valve placed between the pumps and the chamber. The carrier gases (Ar or N<sub>2</sub> in Bordeaux) and excess reagent gases (H<sub>2</sub>, HD and D<sub>2</sub>) are flowed directly from cylinders and mixed upstream of the LN reservoir. As these gases are passed through calibrated mass-flow controllers prior to mixing, the reagent concentrations can be calculated precisely. The precursor molecules used to form specified minor radical reagents are also introduced into reactor upstream of the LN to ensure mixing is complete. The reactive radical species are formed in-situ within the cold supersonic flow through pulsed (10 Hz) laser photolysis of the appropriate precursor molecule. Here, the output beam of a frequency quadrupled Nd:YAG laser at 266 nm is steered into the reactor along its central axis through a ultraviolet (UV) grade quartz window positioned at the Brewster angle to minimize window fluorescence. The beam is coaligned along the length of the supersonic flow and exits the low pressure side of the reactor through the throat of the LN, finally exiting the reactor through a second Brewster angled UV grade quartz window at the back of the reservoir. The beam diameter is reduced to 5-7 mm by a circular diaphragm before entering the reactor to ensure that it can safely pass through the nozzle throat. Typical pulse energies, measured after the reservoir exit window are in the range 20-25 mJ. A small fraction of the UV photons are absorbed by the precursor molecules as they pass through the cold flow, forming the radical reagents directly (C(<sup>1</sup>D), S(<sup>1</sup>D) and O(<sup>1</sup>D)) or indirectly (N(<sup>2</sup>D)).

Table 2 summarizes details (such as precursor molecules used and probe transition wavelengths) specific to studies on individual atomic radicals. C(<sup>1</sup>D) and S(<sup>1</sup>D) were formed by the UV photolysis of CBr<sub>4</sub> and CS<sub>2</sub> precursor molecules respectively, which are commercially available reagents. For experiments employing O(<sup>1</sup>D) atoms, these radicals were generated from ozone (O<sub>3</sub>) photolysis, where O<sub>3</sub> was generated upstream of the reactor. Details of this process can be found in Grondin *et al.* [18]. For studies involving N(<sup>2</sup>D), it was not possible to generate these atomic radicals by direct photolysis at convenient UV wavelengths. Instead, during these experiments, the reaction  $C(^3P) + NO \rightarrow N(^2D) + CO$  was used to generate them chemically [19]. Here, CBr<sub>4</sub> was used as the source of C(<sup>3</sup>P) atoms with a yield of around 85-90 %

Table 2. Precursor molecules, probe laser transitions and wavelengths.

Excited state radical	C( <sup>1</sup> D)	C( <sup>1</sup> D)	N( <sup>2</sup> D)	S( <sup>1</sup> D)
Precursor molecule	CBr <sub>4</sub>	O <sub>3</sub>	CBr <sub>4</sub> /NO (see text)	CS <sub>2</sub>
Photolysis wavelength / nm	266 nm	266 nm	266 nm	193 nm
Probe transition	$1s^2S_{1/2} \rightarrow 2p^2P_{1/2}$	$2s^22p^4^1D_2 \rightarrow 2s^22p^3(^2D)3s^1D_2$	$2s^22p^3^2D_{5/2} \rightarrow 2s^22p^2(^3P)3d^2F_{7/2}$	$3s^23p^4^1D_2 \rightarrow 3s^23p^34s^1D_2$
Probe wavelength /nm	H( <sup>2</sup> S) 121.567 D( <sup>2</sup> S) 121.534	115.215	116.745	166.67

following photolysis at 266 nm according to earlier measurements [20] performed under similar conditions. Consequently, the N(<sup>2</sup>D) atoms generated by this reaction are not formed instantaneously, but at a rate governed by the excess NO concentration. As N(<sup>2</sup>D) atoms also react rapidly with NO [21] the choice of the NO concentration values is critically important to ensure that N(<sup>2</sup>D) atom production is completed on an appropriate timescale (so a high enough [NO] to allow all C(<sup>3</sup>P) atoms to be consumed within a few tens of microseconds) while limiting additional N(<sup>2</sup>D) losses through the N(<sup>2</sup>D)+NO reaction.

Although the detection schemes for individual experiments vary for different radical reagents, a common method is employed for all of the studies described here, namely pulsed laser induced fluorescence. A tunable probe laser in the vacuum ultraviolet (VUV) range, where many strong transitions of these atomic radical reagents lie, is tuned to one of these transitions and directed into the reactor at right angles to the supersonic flow at the level of the observation axis. The VUV radiation is absorbed by the excited state atomic radicals present within the flow that rapidly relax back to the initial excited state by emitting a photon ‘on-resonance’ which is detected by a VUV sensitive photomultiplier tube (PMT). Details of the four wave mixing procedure used to generate tunable VUV radiation to probe S(<sup>1</sup>D) atoms can be found in Lara *et al.* [22], while for the other experiments described here, the VUV probe laser is generated by frequency tripling in rare gases. Here, a frequency doubled Nd:YAG laser at 532 nm is used to pump a dye laser operating in the red region of the electromagnetic spectrum, specifically between 690 and 730 nm. This beam is injected into a Beta Barium Borate (BBO) crystal to generate UV radiation in the range 345-365 nm by frequency doubling. Two dichroic mirrors optimized for reflection at 355 nm are used to separate the desired UV beam from the fundamental radiation whilst also allowing the red light to be collected by a wavemeter to continuously monitor the wavelength throughout the experiment. Once the UV beam has been separated from the fundamental beam, right angled UV coated prisms are used to steer the UV beam towards the observation axis of the reactor where it is focused into a cell using a plano-convex quartz lens. The cell contains either xenon or krypton to allow VUV light in the ranges 115-119 nm or 120-122 nm to be generated through non-resonant third-order sum-frequency mixing in a negative dispersive rare gas [23]. Furthermore, a positive dispersive rare gas, Ar, was added to the cell to improve the conversion efficiency through phase matching. As the VUV beam exiting the cell is now divergent, a MgF<sub>2</sub> lens is used as the output window to steer the VUV beam into the reactor. In this way, the VUV beam is collimated while the residual UV beam remains divergent

due to the large difference in refractive index of the lens at VUV and UV wavelengths. The cell itself is attached to the reactor through a 75 cm long sidearm containing a series of diaphragms. This setup thereby prevents a large fraction of the divergent UV beam from reaching the reactor and minimizes scattered light detection. As this sidearm is open to the reactor, residual gases rapidly fill it, an issue which could cause significant absorption losses of the VUV probe source before it reaches the cold supersonic flow (losses mostly arise from precursor molecule absorption in these experiments). To avoid this problem, the sidearm is maintained at a slightly positive pressure with respect to the reactor by constantly flushing it with a small flow of Ar or N<sub>2</sub>. As such, losses of the VUV excitation source are kept to a minimum. On the detector side, the PMT is positioned orthogonally to the probe laser, the photolysis laser and the supersonic flow (which is coaxial with the photolysis laser); a configuration that minimizes scattered light from both the probe and photolysis lasers. As the transmission of VUV emission is strongly attenuated by atmospheric O<sub>2</sub> when air is present, the zone between the PMT and the reactor is maintained under vacuum and isolated from the reactor by a LiF window. A LiF lens is also positioned in this evacuated region to focus the emitted light from the supersonic flow onto the photocathode of the PMT. Although this configuration limits the level of VUV light collected by the PMT (due to attenuation of the VUV radiation by the LiF optics), it represents a good compromise between detection sensitivity whilst still protecting the delicate envelope of the VUV sensitive detector. The output of the PMT is fed into a boxcar integration unit which provides the possibility to selectively detect the VUV emission pulse by allowing a gate to be placed around this signal. To follow the kinetics of the reaction under investigation, the time between the photolysis and probe lasers is varied by using a digital delay generator to control the trigger pulses for both of these systems. Similarly, the boxcar integration system is also triggered with the same delay generator to enable easy synchronization of the pulsed detection system. In the present experiments, the photolysis laser pulse creates a column of atomic radicals along the length of the supersonic flow. If the probe laser fires simultaneously, those radicals that are created directly in the observation region are excited and relax by radiating a photon, with the emission being collected by the PMT. In this situation, as the created radicals have had no time to react with the excess hydrogen coreagent species also present in the flow, we observe a maximum in the emitted signal. In contrast, if the probe laser is delayed with respect to the photolysis laser, the radicals created upstream of the observation region have time to react before moving into the observation zone where they are detected, so a lower emitted signal is recorded. If the probe laser is triggered prior to the photolysis laser, no radicals are present in the flow, so this situation presents the ideal opportunity to record the baseline signal consisting of scattered probe laser light (which is on-resonance with the fluorescence emission) and any other spurious emissions and dark noise from the detector itself. In this way, and by varying the time delay systematically over the entire useable length of the supersonic flow, a curve of the temporal evolution of the radical species can be constructed as shown below in Figure 3.

### 2.1. Temperature dependent rate constants

In the case of the  $\text{O}(^1\text{D})+\text{HD}$  reaction, the radical reagent  $\text{O}(^1\text{D})$  is detected so that in the presence of a large excess of HD, the radical reagent decays to zero, following an exponential profile of the type:

$$[\text{O}(^1\text{D})] = [\text{O}(^1\text{D})]_0 e^{-k't}, \quad (1)$$

where  $[\text{O}(^1\text{D})]$  and  $[\text{O}(^1\text{D})]_0$  are the time dependent and initial concentrations of  $\text{O}(^1\text{D})$  respectively and  $k'$  is the sum of all first-order losses of  $\text{O}(^1\text{D})$ . In the absence of secondary losses for  $\text{O}(^1\text{D})$ ,  $k' = k_{\text{O}(^1\text{D})+\text{HD}}[\text{HD}]$ . When the excess coreagent concentrations are large, the pseudo-first-order (PFO) decay rates are faster than those recorded for low or zero coreagent concentrations. Nevertheless, in the absence of coreagent species, the radical reagent still decays exponentially to zero, albeit at a slower rate meaning that the measured  $k'$  is due to several different processes. In the case of excited electronic state atomic radicals such as  $\text{O}(^1\text{D})$  this occurs due to a combination of several effects including reactive losses ( $\text{O}(^1\text{D}) + \text{O}_3 \rightarrow 2 \text{O}_2$  with a rate constant  $k_{\text{O}(^1\text{D})+\text{O}_3}$ ) and non-reactive quenching losses with precursor molecules

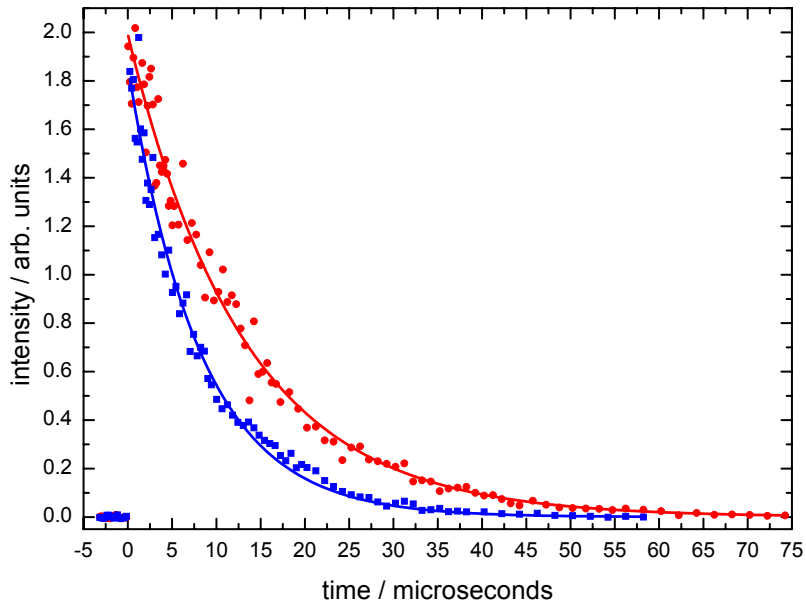


Figure 3.  $\text{O}(^1\text{D})$  VUV LIF signal as a function of delay time between the photolysis and probe lasers recorded at 127 K during an investigation of the  $\text{O}(^1\text{D}) + \text{HD}$  reaction. Signal obtained without HD and the  $\text{O}(^1\text{D})$  VUV LIF signal decays due to quenching collisions with the carrier gas Ar (Red solid circles), and with  $[\text{HD}] = 3.4 \times 10^{14} \text{ cm}^{-3}$ . Solid lines represent single exponential fits to the individual datasets (blue solid squares).

( $O(^1D) + O_2 \rightarrow O(^3P) + O_2$  with a rate constant  $k_{O(^1D)+O_2}$ ), but mostly due to non-reactive quenching losses with the carrier gas molecules ( $O(^1D) + Ar \rightarrow O(^3P) + Ar$  with a rate constant  $k_{O(^1D)+Ar}$ ). Consequently, it can be written that

$$k' = k_{O(^1D)+HD}[HD] + k_{O(^1D)+O_3}[O_3] + k_{O(^1D)+O_2}[O_2] + k_{O(^1D)+Ar}[Ar] + k_L \quad (2)$$

where  $k_L$  represents any other losses of  $O(^1D)$  atoms such as diffusion. As the precursor molecules  $O_3$ ,  $O_2$  and carrier gas  $Ar$  concentrations are fixed for any single series of measurements, the observed change in PFO decay rate is solely due to the change in excess coreagent concentration. In other situations, such as during kinetic measurements of  $C(^1D)$  radical reactions with hydrogen and its isotopologues, it was not possible to detect  $C(^1D)$  directly as no favorable transitions were available for this radical in the various detection windows provided by the rare gas tripling method employed in Bordeaux. Instead, it was possible to study the kinetics of the  $C(^1D)$  reaction by following the  $H(^2S)$  or  $D(^2S)$  products formed by these reactions, giving rise to emission profiles such as those shown in Figure 4.

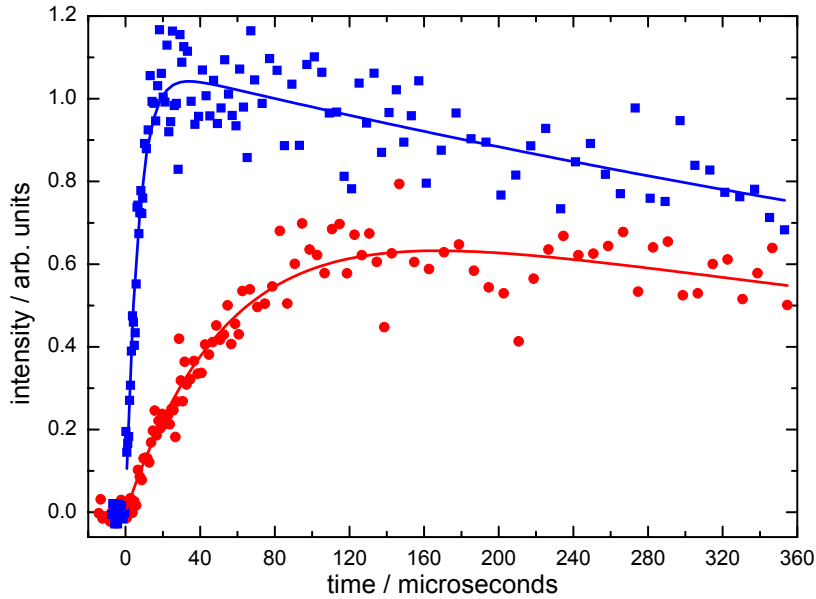


Figure 4.  $D(^2S)$  atom formation curves from the  $C(^1D) + D_2 \rightarrow CD + D$  reaction recorded at 50 K for  $[D_2] = 6.8 \times 10^{14}$  molecule  $cm^{-3}$  (Blue solid squares) and  $[D_2] = 6.0 \times 10^{13}$  molecule  $cm^{-3}$  (red solid circles). Solid lines represent biexponential fits to the data of the form given by equation (1).

Temporal profiles of this type can be analysed using a function of the form

$$[D] = [D]_0 \left( e^{-k_{L(D)}t} - e^{-k't} \right) \quad (3)$$

where  $[D]$  and  $[D]_0$  are the time dependent and peak D-atom concentrations (which are considered to be proportional to the recorded emission signal),  $k_{L(D)}$  represents the combined first-order losses of D-atoms such as through diffusion or secondary reactions and  $k'$  is the PFO rate constant for D atom formation (or alternatively, for C(<sup>1</sup>D) atom loss) defined as  $k' = k[D] + k_{L(D)}$ , potentially comprising several terms as described above. It should be noted here that kinetic profiles where the excess coreagent species is absent cannot be determined using this method as the product species (D-atoms in this instance) are not formed. Consequently, such experiments are typically performed over a smaller range of coreagent concentrations.

Generally speaking, the first method (producing temporal profiles such as shown in Figure 3) is preferred for the determination of PFO rate constants if possible, as fits of the type shown in Figure 4 introduce an extra fitting parameter into the analysis leading to substantially larger uncertainties in the derived PFO rates. Secondary losses (chemical or otherwise) of the product species contribute further uncertainty to the derived PFO rate constants for the target reaction. A plot of the PFO rate constants (derived from fits such as those shown in Figures 3 and 4) against the corresponding coreagent concentrations, yields the second-order rate constant from the slope as shown in Figure 5.

In the case of N(<sup>2</sup>D) experiments, the temporal evolution of N(<sup>2</sup>D) atoms should also be described by the biexponential function given by expression (3). In reality, however, as saturation of the preamplifier during the first 15 microseconds following the photolysis laser pulse prevented us from recording the rising part of the temporal profile, the usual exponential decay given by expression (1) was used instead to analyze these data. In this situation, an additional decay due to the N(<sup>2</sup>D) + NO reaction (given by  $k_{N(^2D)+NO} [NO]$ ) contributes to the overall PFO decay rate  $k'$ . Nevertheless, as  $[NO]$  remains constant for any single series of measurements, this additional loss simply adds to the y-axis intercept value of plots similar to those shown in Figure 5. As N(<sup>2</sup>D) losses brought about by the N(<sup>2</sup>D) + NO reaction are generally much more important (values around a few tens of thousands s<sup>-1</sup>) than those brought about by diffusion losses or secondary reactions (values around a few thousand s<sup>-1</sup>), this additional contribution generally leads to somewhat larger uncertainties on the second-order rate constants derived from the slopes of such plots.

Finally, the second-order rate constants are plotted as a function of temperature, to be compared with the theoretical results and earlier studies when these are available. One should realize that the derived values actually represent upper limits for the reactive rate constant, as the extent of the non-reactive quenching process (for example C(<sup>1</sup>D) + D<sub>2</sub> → C(<sup>3</sup>P) + D<sub>2</sub>) cannot be quantified by following the minor reagent losses, although studies of H- (D-) atom product formation can provide some information. Test experiments performed during a study of the C(<sup>1</sup>D) + H<sub>2</sub> reaction by Hickson *et al* [24] suggest that these losses are very minor compared to the reactive ones. Of course, this might not be the case for the equivalent reactions of O(<sup>1</sup>D),

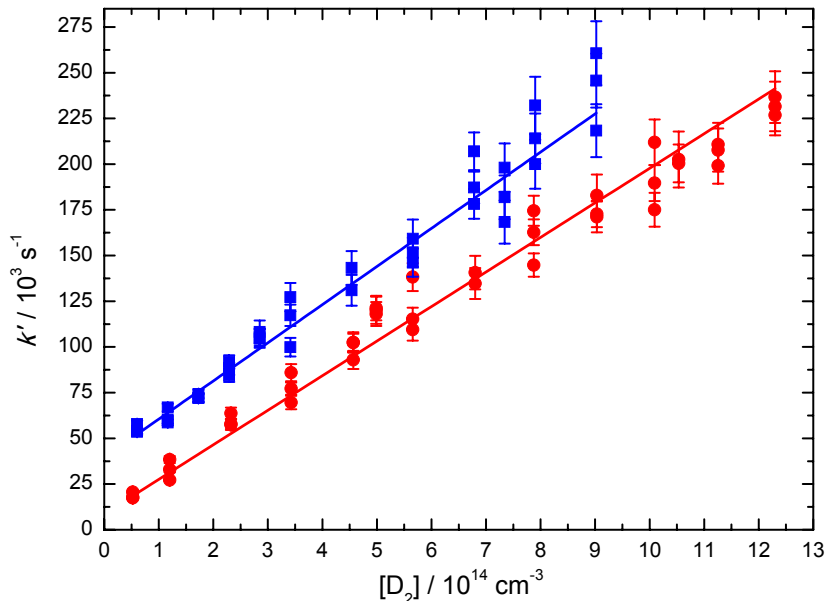


Figure 5. Pseudo-first order rate constants for the  $C(^1D) + D_2$  reaction as a function of  $[D_2]$ , recorded at 296 K (red solid circles) and at 50 K (blue solid squares). The data at 50 K have been shifted upwards by  $40000 \text{ s}^{-1}$  for clarity. Error bars represent the statistical uncertainties of the PFO rate constants derived from biexponential fits given by equation 3. Second-order rate constants were determined by weighted fits to the data.

$N(^2D)$  and  $S(^1D)$ , so this remains an open issue to be resolved in future work. One other factor to consider when comparing with theory is the rotational distributions of  $H_2$  and  $D_2$  in the experiments. Due to inefficient spin conversion between the ortho and para states of these isomers in the reactor as the room temperature gases are expanded through the LN, the room temperature populations of ortho/para- $H_2$ (- $D_2$ ) are retained in the low temperature experiments. Nevertheless, within any single rotational (ortho or para) manifold, collisions with the carrier gas molecules are expected to redistribute the populations to attain thermal equilibrium. For example,  $D_2$  used in these experiments is characterized by a fixed ortho/para ratio of 2 / 1 at all temperatures (the equilibrium value at 300 K). This can be contrasted with the expected equilibrium value at 50 K, which should approach 4 / 1. For  $H_2$ , the room temperature ortho/para ratio of 3 / 1 is preserved in these experiments, while the equilibrium value is close to 1 / 3 at 50 K. Consequently, when comparing theory with experiment it is important to consider the  $j$ -dependent reactivity of the individual rotational levels. Indeed, if a dependence is predicted then the overall theoretical rate constants used to compare with the measured values should accurately reflect the non-equilibrium populations of the experiments rather than the usual thermal values.

## 2.2. Product branching ratios

The reactions of  $C(^1D)$  and  $O(^1D)$  with HD represent an excellent opportunity to provide an in-depth comparison between theory and experiment, due to the possibility for each of these processes to occur via two different product channels.

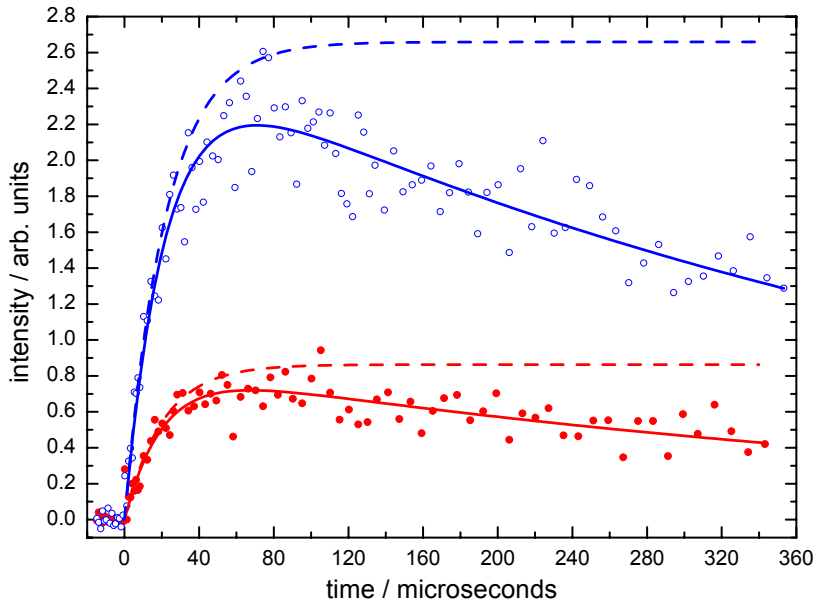


Figure 6. D-atom VUV LIF profiles recorded at 50 K with D-atom signal from the  $C(^1D) + HD$  reaction ( $[HD] = 1.90 \times 10^{14} \text{ cm}^{-3}$  (Red solid circles) and D-atom signal from the  $C(^1D) + D_2$  reaction with  $[D_2] = 2.23 \times 10^{14} \text{ cm}^{-3}$  (Blue solid circles). Solid lines represent biexponential fits to the individual datasets. Dashed lines represent the theoretical D-atom yields without competing D-atom losses.



In this situation, quantitative product yields are most easily obtained by following the atomic (H or D) coproduct as the molecular coproduct will be formed over a range of rovibrational states and therefore difficult to quantify. Under conditions where non-reactive losses of the minor reagent X species are small (such as during  $C(^1D)$  kinetics studies where quenching with the carrier gas Ar is negligible [25]), H-(D)-atom product yields could be obtained as a function of temperature, by recording the time-dependent H-(D)-atom signal intensities of the  $C(^1D) + HD$  target reaction by comparing with the ones obtained from the  $C(^1D) + H_2(D_2)$  reference reaction

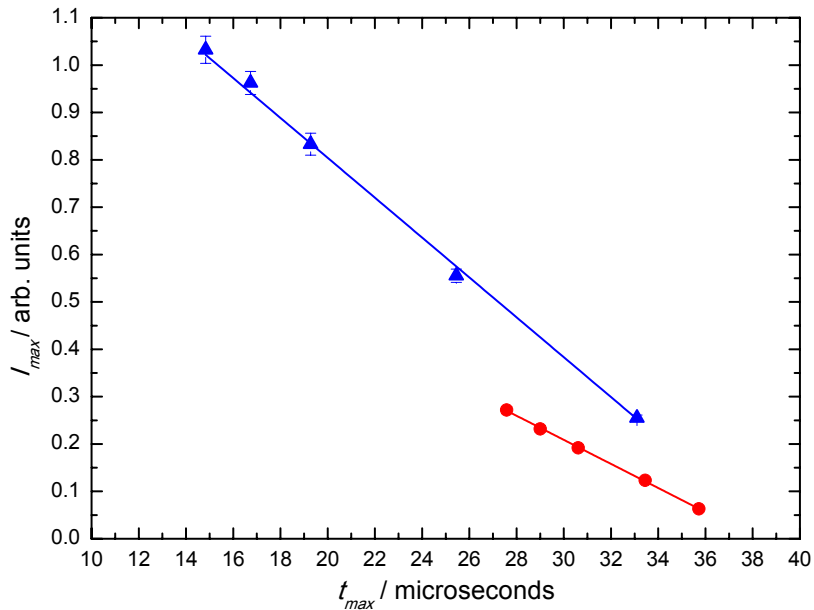


Figure 7.  $I_{max}$ , as a function of  $t_{max}$ , at 127 K; (blue triangles) reference  $O(^1D) + H_2$  reaction; (red circles) target  $O(^1D) + HD$  reaction. Solid lines represent weighted fits to the individual data based on the standard error derived from an average of the recorded intensities at each value of  $t_{max}$ .

with an assumed H-(D-)atom yield of 100% [24, 26]. To ensure that H-(D-)atom losses such as those described in expression (3) above did not lead to errors in the absolute yields, the HD and  $H_2$  ( $D_2$ ) concentrations were adjusted to obtain temporal profiles with similar values of  $k'$ . Several pairs of H-(D-)atom curves were recorded at each temperature to lower the experimental uncertainties. Additionally, the order in which the curves were acquired was inverted alternately to account for potential variations in the fluorescence intensities as a function of experiment time. A pair of  $D(^2S)$  temporal profiles recorded sequentially for the  $C(^1D) + HD$  target and  $C(^1D) + D_2$  reference reactions at 50 K are shown in Figure 6.

Biexponential fits to these curves yield values for the signal amplitude  $-[D]_0$  in expression (3)- representing the theoretical D-atom yield in the absence of competing losses. As HD,  $H_2$  and  $D_2$  absorb only negligibly around 121 nm, it was not necessary to account for absorption losses of the VUV excitation and fluorescence intensities during these experiments. Consequently, absolute D-atom yields were obtained directly by dividing the signal amplitude factors of the target and reference reaction D-atom formation curves.

Unfortunately, in the case of the  $O(^1D) + HD$  target reaction,  $O(^1D)$  quenching by Ar [18] is much more efficient than the equivalent process for  $C(^1D)$  atoms. Consequently, during our investigation of the H-(D-)atom yields, any small discrepancies

in the H-(D-)atom formation rates for the target and reference  $\text{O}(^1\text{D}) + \text{H}_2/\text{D}_2$  reactions could lead to significantly different non-reactive losses for  $\text{O}(^1\text{D})$  atoms. This in turn could induce large errors in the H-(D-)atom yields. An alternative method to circumvent this problem has been described by Nuñez-Reyes *et al.* [27]. Here, the production of H-(D-) atoms from the target  $\text{O}(^1\text{D}) + \text{HD}$  reaction was measured relative to the reference  $\text{O}(^1\text{D}) + \text{H}_2$  ( $\text{D}_2$ ) reaction which is considered to produce H-(or D-) atoms with a 100 % yield. In this case, the experiments measured the peak H- or D- atom fluorescence signal,  $I_{\text{max}}$ , for a range of coreagent concentrations for both the target and reference reactions. The time corresponding to the peak intensity,  $t_{\text{max}}$ , representing the delay between photolysis and probe lasers was calculated prior to the experiments using the expression:

$$t_{\text{max}} = \frac{1}{k_{\text{L(H)}} - k'} \ln \left( \frac{k_{\text{L(H)}}}{k'} \right) \quad (6)$$

where  $k'$  values were obtained through kinetic experiments following  $\text{O}(^1\text{D})$  loss, while  $k_{\text{L(H)}}$ , the diffusional loss rate for H-(D-) atoms, was obtained from previous experiments performed under similar conditions. A typical pair of plots of  $I_{\text{max}}$  versus  $t_{\text{max}}$  recorded at 127 K for the target and reference reactions is shown in Figure 7. As absorption losses by HD,  $\text{H}_2$  or  $\text{D}_2$  are negligible, a ratio of the slopes of these plots then leads directly to the H-(D-) yield of the reaction.

### 3. Theory for complex-forming reactions

Along the years, different approaches designed to treat complex-forming reactions have been applied in the context of the  $\text{X} + \text{H}_2$  processes treated in this work. The theoretical foundation of these methods and the corresponding numerical considerations regarding their application to a number of different atom-diatom reactions were already detailed before [10, 28–41], so here we will restrict ourselves to the most relevant features for treating the kinetics at low temperature. The exact quantum dynamics investigation of processes mediated by the presence of a relatively deep potential well between reactants and products usually implies a significant computational effort. Statistical and capture theories constitute an interesting alternative despite their approximate nature. All the four reactions grouped in this review share in common the existence of a ground electronic state with a deep potential well in the intermediate region. The overall dynamics of the processes occurs mainly on this sole ground potential energy surface and therefore most of the statistical calculations shown here have been performed only this surface. Only in some cases where stated, the contribution from an excited electronic state is taken into account. In this section, we summarize those approaches employed in our recent research at the low temperature regime for the reactive collisions between molecular hydrogen and  $\text{C}(^1\text{D})$ ,  $\text{N}(^2\text{D})$ ,  $\text{O}(^1\text{D})$  or  $\text{S}(^1\text{D})$ .

### 3.1. Statistical quantum method

One of the techniques employed to study the dynamics of the X+H<sub>2</sub> reactive collisions treated in the present review is the statistical quantum method (SQM) developed by Manolopoulos and coworkers [9, 42]. The method assumes a complex-forming mechanism ruling the overall dynamics of the process and separates the formation and fragmentation of the intermediate species in the course of the reaction between reactants and products, as independent events. Individual capture probabilities for both processes are then calculated using a full *ab initio* potential energy surface (PES) setting a capture radius both at the entrance of the reactant channel and at the exit product channels which define the region where the collision complex is assumed to be formed. The actual calculation is performed between the region defined by each capture radius and the asymptotic region, neglecting the intermediate region of the PES, which leads to a statistical distribution of the long-lived complex states as a result of the substantial depth of the potential well. In the original version of the SQM method [9, 42], a time independent quantum mechanical (TIQM) calculation by means of a log derivative method was performed in order to obtain the individual probability for the collision complex to form from the diatom reactant rovibrational state  $(v, j, l)$  at a specific value of the total angular momentum  $J$  and the total energy  $E$ ,  $p_{vjl}^J(E)$  and for its fragmentation onto the final product reactant state  $(v', j', l')$ ,  $p_{v'j'l'}^J(E)$ . In some other versions of this method, such a calculation is performed by means of either a quasi-classical trajectory (QCT) [43–45] or time dependent wave packet (TDWP) propagation [46]. With these capture probabilities the state-to-state probability can be approximated as:

$$|S_{vjl, v'j'l'}^J(E)|^2 \simeq \frac{p_{vjl}^J(E)p_{v'j'l'}^J(E)}{\sum_{v''j''l''} p_{v''j''l''}^J(E)}, \quad (7)$$

where the indexes  $v, j, l(v', j', l')$  refer to the vibrational, rotational and orbital angular momentum quantum numbers, respectively for the reactant (product) arrangements and the sum in the denominator runs for all energetically accessible diatom states. With the expression of Eq. (7), product state resolved integral cross sections (ICS) are obtained by means of the standard expression:

$$\sigma_{vj, v'j'}(E) = \frac{\pi}{gk_{vj}^2(2j+1)} \sum_{Jl'l'} (2J+1) |S_{vjl, v'j'l'}^J(E)|^2, \quad (8)$$

with  $k_{vj}^2 = 2\mu(E - E_{vj})/\hbar^2$ ,  $E_{vj}$  being the energy of the initial rovibrational state  $vj$  of the reactant diatom,  $\mu$  the reduced mass and  $g$  the electronic degeneracy. Finally, evaluating the ICS of Eq. (8) as a function of the collision energy,  $E_c = E - E_{vj}$ , we can calculate the rate constants as:

$$k_{vj, v'j'}(T) = \sqrt{\frac{8\beta^3}{\pi\mu}} \int_0^\infty \sigma_{vj, v'j'}(E) E_c e^{-\beta E_c} dE_c, \quad (9)$$

where  $\beta = (k_B T)^{-1}$ .

### 3.2. Mean potential phase space

Mean potential phase space theory (MPPST) is a slight extension of phase space theory (PST) [36, 37, 47–50]. Instead of using the isotropic approximation  $-C_n/R^n$  for the inter-fragment potential as in PST ( $R$  is the distance between the atom and the center-of-mass of the diatom), one uses, in each channel, the average over the Jacobi angle of the exact potential energy of interaction between the atom and the diatom taken at its equilibrium geometry. The theory involves the same expressions as SQM - see Eqs. (7)-(9), except that the calculation of capture probabilities is simplified: when ignoring tunneling, these are equal to 1 or 0 depending on whether the top of the centrifugal barrier is lower or higher than the collision energy (the centrifugal barrier results from the sum of the attractive angle-averaged potential energy and the repulsive centrifugal energy). Diatom and orbital rotational motions can be treated classically except when few asymptotic states are available. In such a case, these motions must be semi-classically quantized in order to improve the quality of the predictions. Tunneling through the centrifugal barrier can also be accounted for by means of a standard WKB treatment [40, 51]. This is what we have done for the results presented in this review.

### 3.3. Mean potential capture theory

Mean potential capture theory (MPCT) is the extension of MPPST in the limit where the formation of the intermediate complex is followed by that of the product species with nearly unit probability [35, 52, 53]. This happens, within the statistical approximation, whenever the amount of available product states is much larger than that of the reagents, which is generally so for sufficiently exoergic reactions. The MPCT **total reaction** cross section is then expressed as:

$$\sigma_{vj}(E) = \frac{\pi}{gk_{vj}^2(2j+1)} \sum_{Jl} (2J+1)p_{vjl}^J(E). \quad (10)$$

The rate constant  $k_{vj}(T)$ , deduced from the above expression, is given by Eq. (9) with  $\sigma_{vj}(E)$  substituted for  $\sigma_{vj,v'j'}(E)$ . These quantities are not product-state resolved, contrary to those given by Eqs. (8) and (9), but they are easier to calculate.

### 3.4. Semiclassical capture theory

The  $\text{N}(^2\text{D})+\text{H}_2$  and  $\text{D}_2$  reactions exhibit an entrance barrier and a strong exoergicity. The existence of the barrier, revealing the importance of short range forces, makes useless the previous models for capture based on isotropic interaction potentials. Alternatively, quasi-classical trajectory calculations may be used. Semiclassical capture (SCC) theory involves the same expressions as MPCT but the capture probability  $p_{vjl}^J$  is computed by running the set of classical trajectories corresponding to quantum numbers  $(v, j, l, J)$  from the reagents towards the well, thus accounting for all the couplings between the degrees of freedom in the entrance channel. Some trajectories reach it, some others do not as they bounce back at a given turning point along the  $R$  coordinate before entering the well. The probability that such paths tunnel through

the barrier is then computed from the turning point by means of the WKB formula [38].

One should note that statistical models are not able to describe the details of state-to-state observables such as state-resolved DCS or  $J$ -resolved reaction probabilities oscillatory patterns, in particular in the quantum regime, i.e. when very few states of the reactants and products are available. This originates from the fact that the statistical models do not account for the correct Poisson distribution for S matrix element and possible incomplete quenching of the interferences.[54, 55] However, as far as integral cross-sections or rate constants (of interest in the present work) are concerned, statistical approaches are expected to be valid.

#### 4. $C(^1D)+H_2$

An intense activity over the past few years on the theoretical side has led to the development of a number of different PES to describe the interactions which govern this reaction on the ground electronic state  $1^1A'$  [56–61]. This surface is characterized by the presence of a deep potential well ( $\approx 4.29$  eV) responsible for an overall complex-forming dynamics at the low energy regime. One of the most recent examples is the *ab initio* ZMB-a surface developed by Zhang *et al.* [61] which includes an accurate description both of the barriers induced by the conical intersection existing between the  $1^1A'$  and  $2^1A'$  states at the HCH and CHH linear configurations, and of the van der Waals (vdW) wells at the entrance and exit channels. The differences with previous PESs, such as that reported in Ref. [57] (the so called RKHS PES) which was a refinement of the BHL surface by Bussery *et al.* [56], were manifested in noticeable discrepancies between the dynamics observed at low collision energies in both cases. The ZMB-a surface has been employed in the real wave packet (WP) calculation performed in Ref. [62] for both the  $C(^1D)+H_2$  and  $C(^1D)+D_2$  reactions and on the QCT investigation reported by Zhang *et al.* [61] for the  $C(^1D)+H_2$  case.

The description of the electronically excited states has also been of importance given their contribution on the overall dynamics of the  $C(^1D)+H_2$  reaction. On the one hand, the contribution from the first excited electronic state  $1^1A''$  state yields a direct sideways insertion mechanism as opposed to the indirect perpendicular approach of the C atom found for the lower ground state in the WP calculation by Defazio *et al.* [63]. Indeed, values of the rate constants for the  $C(^1D)+H_2/D_2/HD$  reactions are also found to be affected by the contribution from this excited state [24, 26, 64–66]. On the other hand, the use of the PES developed by Bussery-Honvault *et al.* [67] for the  $1^1A''$  state, did not improve the comparison between theoretical simulations of laboratory angular and TOF distributions [7] and, in contrast, the agreement seemed to be worse than when only the ground electronic state was employed in the calculations. In a more recent study, Shen *et al.* [68] constructed an accurate global analytical PES (ZMB-b) for the same excited electronic state. Quantum dynamic calculations employing both the ZMB-a and ZMB-b PESs for the ground  $1^1A'$  and excited  $1^1A''$  electronic states produced product vibrational branching ratio functions in a much better agreement with a CMB experiment on the  $C(^1D)+D_2$  reaction [8] than any other calculation performed solely on the ground state. In addition to this,

Wu *et al.* [69] showed the importance of a good description of a conical intersection between excited electronic states which induces a bond-selective activation influencing the product branching ratios of the  $C(^1D)+HD$  reaction.

Different measurements of rate constants  $C(^1D)+H_2$  [65, 70, 71],  $C(^1D)+D_2$  [65, 70] and  $C(^1D)+HD$  [65] reactions have been previously reported in the literature. More recent kinetics investigations [24, 26, 69] have yielded rate constants for the  $C(^1D)+H_2/D_2/HD$  reactions over the 50-300 K range obtained with the Bordeaux supersonic flow reactor. Combined with this effort from the experimental side, numerous theoretical calculations have also produced rate constants by means of a series of numerical techniques such as ring-polymer molecular dynamics (RPMD) [24, 26], real WP [63, 64, 72] and QCT [73].

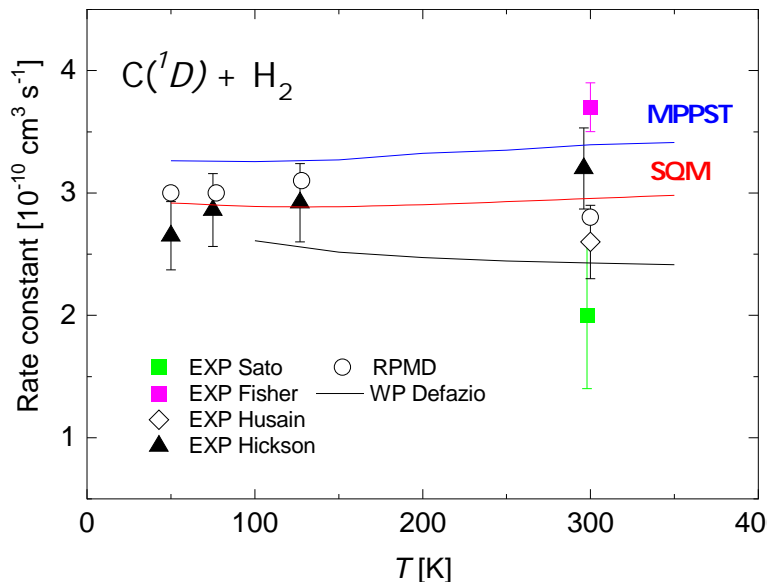


Figure 8. Rate constants for the  $C(^1D)+H_2$  reaction measured in  $10^{-10} \text{ cm}^3 \text{ s}^{-1}$ . Experimental results are from Hickson *et al.* [24] (black triangles), Sato *et al.* [65] (green squares), Fisher *et al.* [70] (magenta squares) and Husain *et al.* [71] (open diamonds). Theoretical results are: MPPST (blue line) and SQM (red line) values are from Ref. [34], WP (black line) are from Defazio *et al.* [63] and the RPMD values (open circles) are from Ref. [24]. All calculations were performed considering contributions from both the ground  $1^1A'$  and first excited  $1^1A''$  electronic states.

The importance of complex-forming mechanisms on the overall dynamics of the process has been highlighted on several occasions. Thus, for example, the good performance of thermally averaged statistical predictions to describe adequately the rotational distributions in the vibrational ground state  $CH(v' = 0)$  obtained in a laser-induced fluorescence (LIF) experiment [74] was explained in terms of the formation of an intermediate species  $CH_2$  with a lifetime of the order of picoseconds [74, 75]. The assumption of the formation of a collision complex after the insertion of

a C atom into the H-D bond was also considered in the RRK calculation [70] which reproduced the observed CD/CH branching ratios [65, 70]. Analogously, the qualitative agreement between PST predictions and CMB experiments for both product angular and TOF distributions led Bergeat *et al.* [76] to conclude that the C(<sup>1</sup>D)+H<sub>2</sub> reaction behaves nearly statistically. Reaction probabilities with numerous narrow peaks obtained in QM calculations reveal that the overall dynamics of the process is mediated by the presence of long-lived resonances [56, 77, 78] and the symmetry observed for angular differential cross sections (DCS) with respect to the forward ( $\theta \sim 0^\circ$ ) and backward ( $\theta \sim 180^\circ$ ) scattering directions reinforced the possibility of a dominating insertion pathway [7, 79]. Collision time distributions estimated by means of the QCT calculation reported in Balucani *et al.* [7] were also consistent with the existence of long-lived intermediate complexes. More recently, Shen *et al.* [80] pointed out the preference for the formation of CH in its ground vibrational state CH( $v = 0$ ), the inversion of the product rotational distributions and a pronounced forward-backward symmetry in the DCS as indicators of such insertion dynamics for C(<sup>1</sup>D)+H<sub>2</sub>. Similar symmetrical angular distributions were found for the case of C(<sup>1</sup>D)+D<sub>2</sub> [68].

These considerations encouraged the application of the SQM approach [8–10, 34, 42], of its WP version [81, 82] and MPPST [35–37, 83] to the study of the C(<sup>1</sup>D)+H<sub>2</sub> reaction and its isotopical variants with fairly good results. One of the most recent examples of an investigation performed with such statistical techniques can be found in Ref. [34].

Here we show in Figure 8 the comparison between our rate constants obtained experimentally for the C(<sup>1</sup>D)+H<sub>2</sub> reaction with a number of different studies and the predictions we have obtained by means of the MPPST and SQM methods for values of the temperature between 50 K and 350 K. Whereas measurements of the rate constant at room temperature ( $T \sim 298$  K) lie within the range defined between the value reported by Sato *et al.* [65] ( $2 \times 10^{-10}$  cm<sup>3</sup> s<sup>-1</sup>) and that by Fisher *et al.* [70],  $(3.7 \pm 0.2) \times 10^{-10}$  cm<sup>3</sup> s<sup>-1</sup>, with the measurement by Husain *et al.* [71] in between, the results measured by one of us [24] at four different temperatures display a slight increase from  $(2.65 \pm 0.28) \times 10^{-10}$  cm<sup>3</sup> s<sup>-1</sup> at 50 K to  $(3.2 \pm 0.33) \times 10^{-10}$  cm<sup>3</sup> s<sup>-1</sup> at 296 K. Both statistical predictions (especially the SQM values) obtained using the RKHS PES (<sup>1</sup>A' + <sup>1</sup>A'') states reproduce well the experimental measurements. The WP results reported by Defazio *et al.* [63], also calculated employing the ground and first excited electronic states, remain below both the measured and the statistical rate constants.

A similar good agreement between our experiment and statistical predictions is found for C(<sup>1</sup>D)+D<sub>2</sub>. SQM rate constants are, as in the case of C(<sup>1</sup>D)+H<sub>2</sub>, slightly lower than those obtained with the MPPST approach. Figure 9 shows the corresponding comparison including the values of  $k(T)$  calculated with RPMD as reported by Hickson *et al.* [26]. Rate constants from the WP calculations of Defazio [63] and Shen [68], also included in Figure 9, are smaller and provide a good theoretical counterpart to measurements from Ref. [26].

For the case of the C(<sup>1</sup>D)+HD reaction the interest also includes the analysis of the branching ratio between the two possible product arrangements, CH + D and CD + H. In Figure 10 we show the comparison between the experimental values of

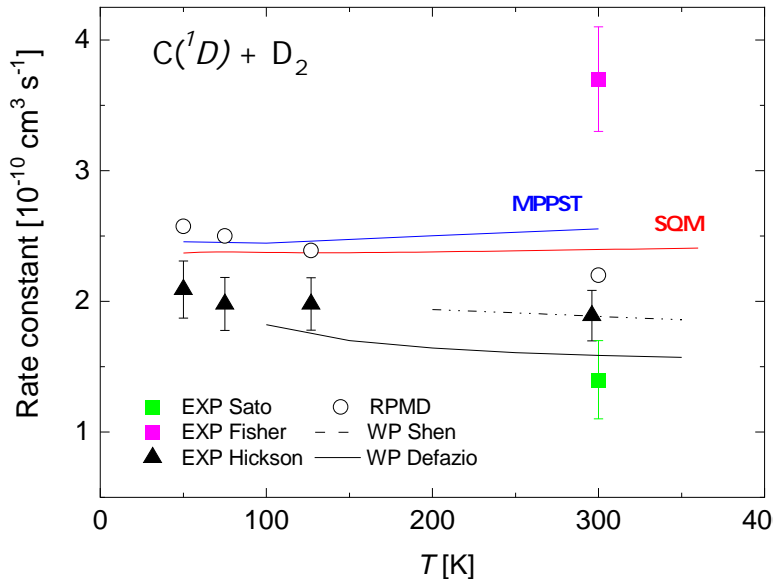


Figure 9. Same as Fig. 8 for the  $C(^1D)+D_2$  reaction. Experimental results are from Hickson *et al.* [26] (black triangles), Sato *et al.* [65] (green squares) and Fisher *et al.* [70] (magenta squares). Theoretical results are: MPPST (blue line) and SQM (red line) values are from González-Lezana *et al.* [34]; the RPMD values (open circles) are from Hickson *et al.* [26] and WP calculations from Defazio *et al.* [63] (solid black line) and from Shen *et al.* [68] (dotted-dashed black line). All calculations were performed considering contributions from both the ground  $1^1A'$  and first excited  $1^1A''$  electronic states.

such CD/CH ratios reported by one these authors in Ref. [69] and our statistical estimates via the SQM and MPPST approaches. MPPST values remaining almost constant around a value of  $\approx 2$  are probably the closest to the experiment, whereas the WP calculation from Wu *et al.* [69], employing the ZMB-a and ZMB-b PESs which take into account the conical intersection between the  $\tilde{b}^1A''$  and  $\tilde{d}^1A''$ , clearly improves those previously reported by Defazio *et al.* [72]

## 5. $N(^2D)+H_2$

The collision between  $N(^2D)$  and molecular hydrogen is expected to play a key role in the chemistry of some planetary atmospheres. In particular, Titan's nitrogen rich atmosphere is composed about 95 % of molecular nitrogen besides traces of some other gases such as molecular hydrogen ( $\sim 0.1\%$ ). Following photolysis of  $N_2$ , the production of significant quantities of  $N(^2D)$  makes the  $N(^2D)+H_2 \rightarrow NH+H$  reaction into the most important source of NH radicals which subsequently take part in the ulterior formation of methanimine ( $CH_2NH$ ) [84].

The presence of a barrier for a collinear geometry  $C_{\infty v}$  [87, 88] besides a deep potential well for the perpendicular  $C_{2v}$  HNH configuration has a profound impact on

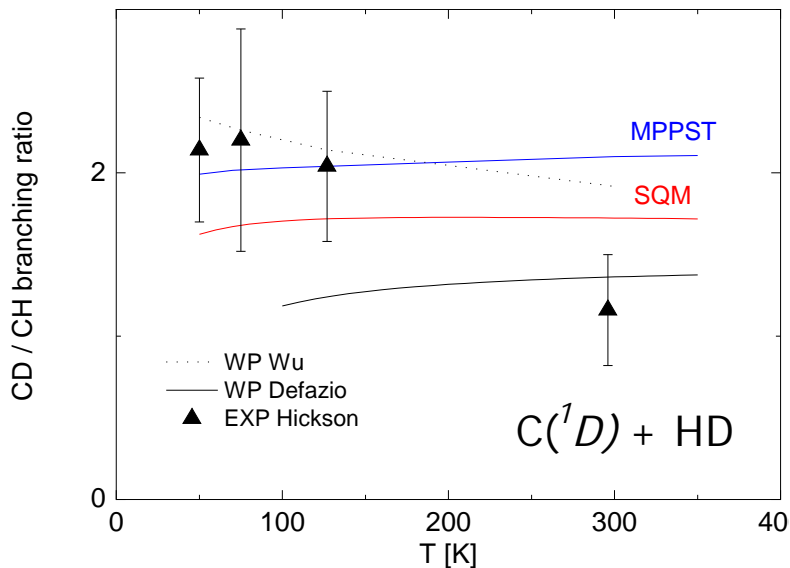


Figure 10. CD/CH Branching ratios for the  $C(^1D)+HD$  reaction. Experimental result is from Hickson *et al.* [69] (black triangles) and theoretical results are: MPPST (blue line) and SQM (red line) values are present work, and WP calculations are taken from Defazio *et al.* [72] (solid black line) and from Wu *et al.* [69] (dotted black line).

the overall dynamics. A good description of such a feature in the corresponding PES [89, 90] is crucial for the understanding of the mechanisms involved in the reaction. After some discussion for a correct interpretation of some product distributions [87, 91–94], it was finally suggested that the dynamics of the  $N(^2D)+H_2/D_2$  reactions corresponds to an insertion mechanism [90, 95–98] with contributions from a direct abstraction pathway when the energy is sufficiently high [99, 100] and contributions from excited electronic states are taken into account [101, 102]. The importance of a complex-forming pathway dominating the process when the reaction proceeds via the ground electronic state was confirmed by the good performance of statistical methods to reproduce QM and experimental rotational and vibrational distributions [10, 36], PTE distributions, laboratory angular distributions and TOF spectra measured by means of a CMB technique [103] and QM DCS [103].

The rate constant of the  $N(^2D)+H_2$  reaction at the room temperature has been measured in the past by means of different techniques [104–111] and values between  $17 \times 10^{-13} \text{ cm}^3 \text{ s}^{-1}$  [105] and  $50 \times 10^{-13} \text{ cm}^3 \text{ s}^{-1}$  [107] have been reported. In particular, we have listed in Table 3 in increasing order, measurements reported by Husain *et al.* [105], Whitefield *et al.* [109], Husain *et al.* [106], Umemoto *et al.* [111], Piper *et al.* [110], Suzuki *et al.* [85], Black *et al.* [107], Fell *et al.* [108] and Black *et al.* [104], in comparison with our recent value reported in Nuñez-Reyes *et al.* [38]. For  $N(^2D)+D_2$ , Umemoto *et al.* [111] provided a value of the rate constant also at room temperature

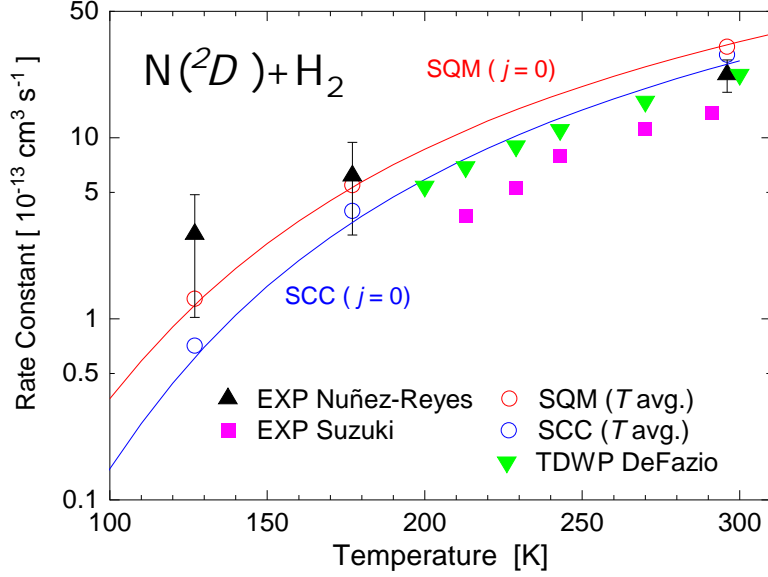


Figure 11. Rate constants for the  $\text{N}(^2\text{D})+\text{H}_2$  reaction. Our experimental results from Nuñez-Reyes *et al.* [38] (black triangles) and those Suzuki *et al.* [85] (magenta squares), in comparison with theoretical results: SCC (blue) and SQM (red) for the  $\text{H}_2(v=0, j=0)$  initial state (solid lines) and at specific values of  $T$  by means of a thermal average involving the most populated  $\text{H}_2(j)$  rotational states at those temperatures (open circles) from our work Nuñez-Reyes *et al.* [38] and the WP calculation from Defazio *et al.* [86] (green triangles), respectively.

of  $1.4 \times 10^{-12} \text{ cm}^3 \text{ s}^{-1}$  in a good agreement with the result obtained before by Suzuki *et al.* [85]. These authors performed a temperature dependent investigation of both  $\text{N}(^2\text{D})+\text{H}_2/\text{D}_2$  reactions, providing values of the rate constants between  $T = 213$  K and 300 K. In this work  $\text{N}(^2\text{D})$  atoms were detected at 149 nm by resonance absorption following the dissociation of  $\text{N}_2$  in the presence of molecular hydrogen by means of a pulsed electron beam [85]. The behaviour of the rate constant was fitted to Arrhenius expressions:  $k(T) = 4.6 \times 10^{-11} \exp(-880/T) \text{ cm}^3 \text{ s}^{-1}$  for  $\text{N}(^2\text{D})+\text{H}_2$ , and  $k(T) = 3.9 \times 10^{-11} \exp(-970/T) \text{ cm}^3 \text{ s}^{-1}$  for  $\text{N}(^2\text{D})+\text{D}_2$ . The SQM approach was employed to investigate the kinetics of the reaction [103] using the PES of Ref. [112] and predictions of both the rate constants for  $\text{N}(^2\text{D})+\text{H}_2$  and  $\text{N}(^2\text{D})+\text{D}_2$ , and of the isotope effect  $\text{NH}/\text{ND}$  were in a fairly good agreement with the experimental values reported by Suzuki *et al.* [85].

Our recent measurement of the rate constants at room temperature [38] for the  $\text{N}(^2\text{D})+\text{H}_2$  reaction ( $22.4 \times 10^{-13} \text{ cm}^3 \text{ s}^{-1}$ ) is in good agreement with previous measurements mentioned above and included in Table 3. Also, as shown in Figure 11 (where we have not included those experimental values at room temperature mentioned before for the sake of clarity) the values measured at some other lower temperatures seem to follow a similar trend as those reported by Suzuki *et al.* [85]. Below room temperature the rate constants reported by us in Ref. [38], reach a value less

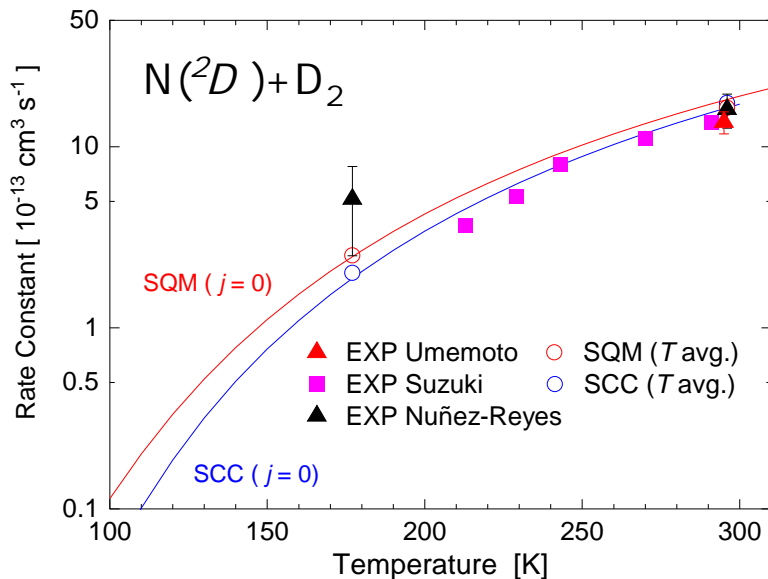


Figure 12. Same as Figure 11 for the  $\text{N}(^2\text{D})+\text{D}_2$  reaction. Our experimental results from Nuñez-Reyes *et al.* [38] (black triangles) are compared with those by Suzuki *et al.* [85] (magenta squares) and by Umemoto *et al.* [111] (red triangles). Theoretical results are SCC (blue) and SQM (red) for the  $\text{D}_2(v=0, j=0)$  initial state (open circles) and by means of an average with the most populated rotational states at  $T=177 \text{ K}$  and room temperature (solid lines) from our work Nuñez-Reyes *et al.* [38].

than  $10^{-12} \text{ cm}^3 \text{ s}^{-1}$ , which is considered to be approaching the limit of measurable reactivity when the Laval nozzle technique is employed. The fit to an Arrhenius expression,  $k(T) = Ae^{-E_a/RT}$ , of the data derived by Nuñez-Reyes *et al.* [38], provides the parameters  $A = 9.5 \times 10^{-12} \text{ cm}^3 \text{ s}^{-1}$  and  $E_a/R = 452 \text{ K}$ , which yield a value of the rate constant at 150 K (considered as a representative for Titan's atmosphere) of  $4.7 \times 10^{-13} \text{ cm}^3 \text{ s}^{-1}$ , about four times larger than the value obtained with the presently recommended Arrhenius fit given in Ref. [113]. The actual comparison is shown in Figure 11 besides the predictions obtained by means of the SQM and the SCC approaches for the case of the reaction with the molecular hydrogen in its ground rotational state  $\text{H}_2(j=0)$ . The latter is found to exhibit a remarkably good accord with the results of the WP calculation by Defazio *et al.* [86]. In addition, at the specific temperatures at which the rate constant has been measured, theoretical estimates are calculated considering an average involving the most populated rotational states.

The value of the rate constant at room temperature for the  $\text{N}(^2\text{D})+\text{D}_2$  reaction measured by Nuñez-Reyes *et al.* [38] is  $16 \times 10^{-13} \text{ cm}^3 \text{ s}^{-1}$ , slightly smaller than the one for the collision with molecular hydrogen, but in a perfectly good agreement with previously reported  $k(T)$  by Umemoto *et al.* [111] and Suzuki *et al.* [85]. As shown in Figure 12, our recent measurements [38] are in an overall good accord

Table 3. Values of **experimental** rate constants (in  $10^{-13} \text{ cm}^3 \text{ s}^{-1}$ ) for the  $\text{N}(^2\text{D})+\text{H}_2/\text{D}_2$  reactions at room temperature in K

$T$	$\text{N}(^2\text{D})+\text{H}_2$	$\text{N}(^2\text{D})+\text{D}_2$	Reference
300	$17.0 \pm 5.0$		Husain <i>et al.</i> [105]
300	$18.0 \pm 8.0$		Whitefield <i>et al.</i> [109]
300	$21.0 \pm 3.0$		Husain <i>et al.</i> [106]
296	$22.4 \pm 4.6$		Nuñez-Reyes <i>et al.</i> [38]
300	$22.8 \pm 2.3$		Umemoto <i>et al.</i> [111]
300	$23.0 \pm 5.0$		Piper <i>et al.</i> [110]
300	$24.4 \pm 3.4$		Suzuki <i>et al.</i> [85]
300	$27.0 \pm 2.0$		Black <i>et al.</i> [107]
300	$35.0 \pm 10.0$		Fell <i>et al.</i> [108]
300	50.0		Black <i>et al.</i> [104]
291		$13.7 \pm 0.7$	Suzuki <i>et al.</i> [85]
295		$13.7 \pm 1.9$	Umemoto <i>et al.</i> [111]
296		$16.1 \pm 3.4$	Nuñez-Reyes <i>et al.</i> [38]

with those from Suzuki *et al.* from Ref. [85], but as  $T$  decreases, the rate constants measured by Nuñez-Reyes *et al.* [38] are somewhat larger. In fact, the value derived at  $T = 177 \text{ K}$ ,  $(5.2 \pm 2.7) \times 10^{-12} \text{ cm}^3 \text{ s}^{-1}$ , remains clearly above the one obtained with the Arrhenius-type fit suggested for data reported by Suzuki *et al.* in Ref. [85]:  $1.6 \times 10^{-12} \text{ cm}^3 \text{ s}^{-1}$ ). Although the uncertainty on the value obtained by Nuñez-Reyes *et al.* is quite large.

Theoretical predictions obtained by means of our SQM and SCC approaches [38] describe well the experimental data existing for the  $\text{N}(^2\text{D})+\text{D}_2$  reaction. In Figure 12 the comparison includes statistical results: (i) for the entire temperature range under consideration (100 K - 310 K) for the reaction initiated from the ground rotational state  $\text{D}_2(j = 0)$  (with solid lines) and (ii) from an average with the populated rotational states at  $T = 177 \text{ K}$  and room temperature. The SCC rate constants are in particularly good accord with measurements by Suzuki *et al.* [85], whereas our SQM results provide a reasonable counterpart to our measured rate constants [38].

## 6. $\text{O}(^1\text{D})+\text{H}_2$

The  $^1A_1$  electronic ground state in the intermediate region between reactants,  $\text{O}(^1\text{D})+\text{H}_2$  and products,  $\text{H} + \text{OH}$ , correlates directly with the water molecule, which makes the reaction one of the most widely studied among the processes contained in this review. Moreover,  $\text{O}(^1\text{D})$  is one of the most common products of the photodissociation of molecules containing oxygen in planetary atmospheres. Its reaction, not only with molecular hydrogen but with water or methane, is the main pathway to form hydroxyl radicals which contribute to ozone destruction in the Earth's atmosphere.  $\text{O}(^1\text{D})$ , formed in the Martian stratosphere by  $\text{CO}_2$  photolysis [114], contributes to its overall stability participating in the formation of OH which finally recycle CO into  $\text{CO}_2$  through the  $\text{OH} + \text{CO}$  reaction [115].

Among the five singlet electronic states produced by the interaction between  $\text{O}(^1\text{D})$  and  $\text{H}_2(X^1\Sigma_g^+)$  only three are non-repulsive. The ground  $1^1A'$  surface correlates adiabatically with reactants and ground state products  $\text{OH}(X^2\Pi)$  and  $\text{H}(^2S)$  [122, 123]

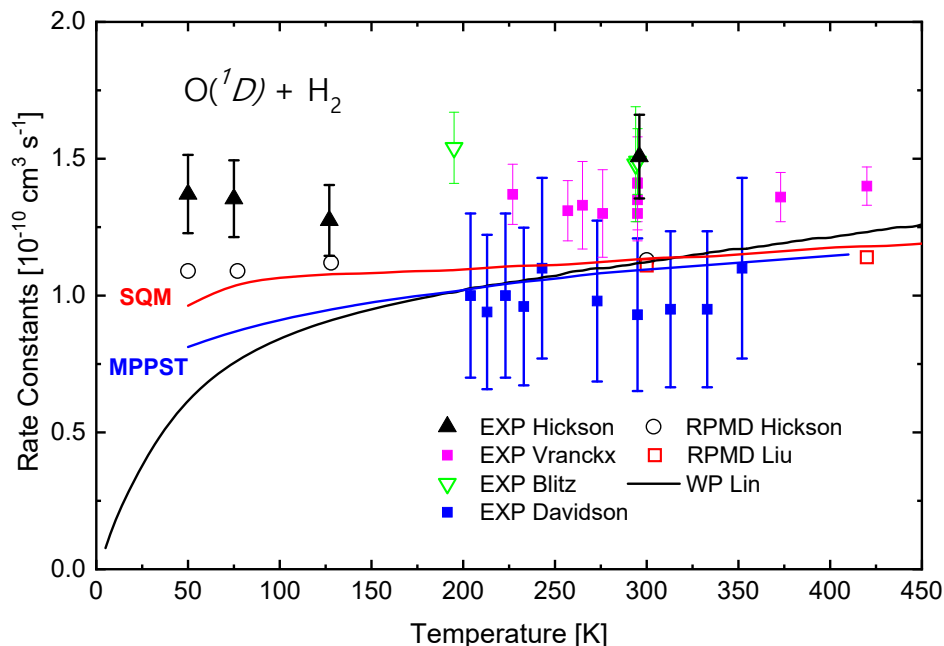


Figure 13. Rate constants for the  $O(^1D)+H_2$  reaction. Experimental results from Hickson *et al.* [116] (black triangles), Vranckx *et al.* [117] (magenta squares), Blitz *et al.* (inverted open triangles) [118], Davidson *et al.* [119] (blue squares) in comparison with theoretical results: MPPST (blue line) and SQM (red line) from Ref.[31], a WP calculation from Lin *et al.* [120] (black line) and the RPMD results from Hickson *et al.* Ref. [116] (empty black circles) and from Liu *et al.* [121] (red open square), respectively.

and displays a deep potential well (about 7.29 eV) which supports a long-lived  $H_2O$  intermediate species. Whereas the dynamics associated to this ground electronic state is found at low energies to correspond to an insertion mechanism with the formation of an intermediate complex between reactants and products [124–127], the contribution from the excited states as the energy increases is seen to introduce an abstraction mechanism [124, 128–131]. In particular, two excited electronic states can also take part in the process: the first excited state  $1^1A''$ , which also correlates adiabatically with the products in their ground state, and the  $2^1A'$  surface which correlates with excited-state  $OH(A^2\Sigma^+)$  and  $H(^2S)$ . Although both states are characterized by the presence of an activation barrier of about 0.104 eV,  $1^1A''$  has no well but  $2^1A'$  has a small potential well (at a lower energy than the separated reactants) and a conical intersection to the ground state  $1^1A'$ . The contribution of this latter excited surface to the reaction takes place through a nonadiabatic pathway. In fact, this possibility, suggested in some theoretical works [120], has been invoked to explain observed differences between experimental rate constants and values obtained in a RPMD calculation [116].

The dynamics of the process and its corresponding deuterated counterparts has been the subject of a number of studies over the years both from the experimental [1, 124, 125, 128, 129, 132–145] and theoretical side [1, 9, 31, 42, 120, 121, 125,

140, 141, 145–159]. The dynamics of the  $O(^1D)+H_2$  reaction at 56 meV collision energy was found to correspond to an insertion process [1, 140], and the comparison of TDWP calculations and Rydberg H-atom TOF spectroscopic measurements on the  $O(^1D)+HD \rightarrow OH+D$  reaction at 74 meV reveals that the ground PES was enough to describe the overall dynamics in terms of a long-lived complex-forming mechanism [160]. However, indications of a transition from a complex-forming dynamics at low energy to an abstraction pathway when the energy increases for  $O(^1D)+D_2$  were found with the analysis of OD product distributions from H(D)-Rydberg 'tagging' TOF experiments at 56 and 139 meV [145]. Also the increase in the backward scattering component of the DCS with the collision energy (86.7-138. meV) observed in the QCT calculation of Ref. [161] was interpreted as the contribution from the  $1^1A''$  PES introducing an abstraction type mechanism.

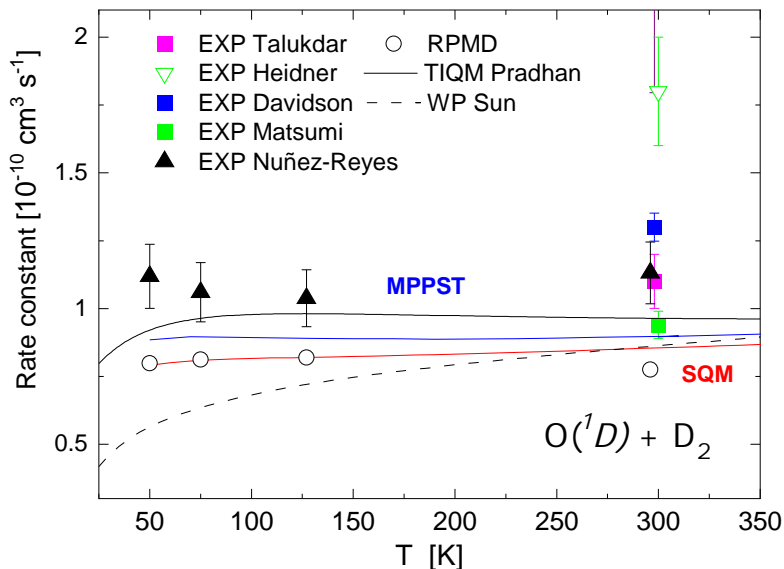


Figure 14. Rate constants for the  $O(^1D)+D_2$  reaction. Experimental results from Ref. [33] (black triangles), Talukdar *et al.* [162] (magenta squares), Heidner *et al.* [163] (inverted open triangles), Davidson *et al.* [119] (blue squares), Matsumi *et al.* [135] (green squares) are compared with theoretical results from MPPST (blue line) and SQM (red line) from Ref.[33], and the WP calculation from Sun *et al.* [164] (black dashed line), the TIQM calculation from Pradhan *et al.* [165] (solid black line) and the RPMD calculation from Ref. [33].

Although most of the previous kinetics measurements were performed close to room temperature [162, 163, 166], the temperature dependence of the  $O(^1D)+H_2$  reaction has also been investigated [117–119]. Those previous investigations have concluded that the reaction is fast, with values of the rate constant usually larger than  $10^{-10} \text{ cm}^3 \text{ s}^{-1}$  and with only weak variations when the temperature remains within the range below 420 K [117–119]. In more recent works, experiments performed using a

supersonic flow reactor coupled with pulsed laser photolysis to produce  $O(^1D)$  and pulsed LIF in the VUV wavelength range yielded values of the rate constants between 50 K and 296 K [33, 39, 116].

Figure 13 shows the rate constants for  $O(^1D)+H_2$  reported from a series of experimental investigations (in particular those by Vranckx *et al.* [117], Blitz *et al.* [118] and Davidson *et al.* [119] and the most recent measurements by one of the present authors [116]) and the theoretical values obtained by means of RPMD [116, 121] and WP calculations [120] between 50 and 430 K. Our experimental rate coefficients look consistent with previous measurements (only slightly larger than those from Davidson *et al.* [119]) and do not display a marked dependence with temperature in the range under study, with values of  $(1.4 \pm 0.1) \times 10^{-10} \text{ cm}^{-1} \text{ s}^{-1}$  at  $T = 50 \text{ K}$  and  $(1.5 \pm 0.1) \times 10^{-10} \text{ cm}^{-1} \text{ s}^{-1}$  at  $T = 296 \text{ K}$  [116], a feature which is fairly well reproduced by our statistical approaches (especially the SQM) and the RPMD calculation of Ref. [116].

Rate constants for the process where  $H_2$  is substituted by the isotopic variant  $D_2$  are also mostly independent with respect to the temperature within the same range. Figure 14 shows the comparison between the measurements recently reported by one of the present authors [33] and previous experimental rate constants at room temperature [119, 135, 163] in comparison with theoretical results. Statistical (both SQM and MPPST), RPMD and TIQM predictions are in good agreement with values from Ref. [33]. Only the WP rates reported by Sun *et al.* [164] exhibit some decreasing behaviour as the temperature decreases, an effect which, on the other hand, is usually observed in this kind of time dependent approach. The comparison, on the other hand, between rate constants for the reactions with  $H_2$  or with  $D_2$  reveals larger values for the  $O(^1D)+H_2$  case. A result which is also observed for the other processes considered in this review. Although the corresponding ICSs for  $O(^1D)+H_2$  and  $O(^1D)+D_2$  are certainly different, the mean velocity of  $H_2$  molecules is larger than the corresponding value for  $D_2$  and hence more collisions in a given time with  $O(^1D)$  are expected and thus a faster rate constant. Moreover, the presence of the reduced mass  $\mu$  (larger for collisions involving  $D_2$ ) in Eq. (9), makes that rate constants for the heavier isotope should be smaller.

Slightly larger discrepancies are seen in the case of the  $O(^1D)+HD$  reaction. Although the accord between experimental and theoretical rate constants is good, with differences not exceeding 30 %, one could argue that the comparison shown in Figure 15 between **our** statistical rate constants obtained with SQM and MPPST calculations and those measured by Nuñez-Reyes *et al.* [39] reveals more noticeable discrepancies than in the above discussed cases of  $O(^1D)+H_2$  and  $O(^1D)+D_2$ . Both approaches yield smaller rate constants than the experiment, whereas the RPMD predictions remain within the error bars.

This is confirmed with the comparison between experimental and theoretical isotopic branching ratios ( $OD+H/OH+D$ ) shown in Table 4. Both SQM and MPPST estimates are almost constant and remain clearly above those obtained from our recent measurements reported in Ref. [39]. RPMD predictions, on the contrary, display similarities with some of the existing experimental branching ratios: As shown in Table 4, at  $T = 50 \text{ K}$ , they agree with our result reported in Nuñez-Reyes *et al.*

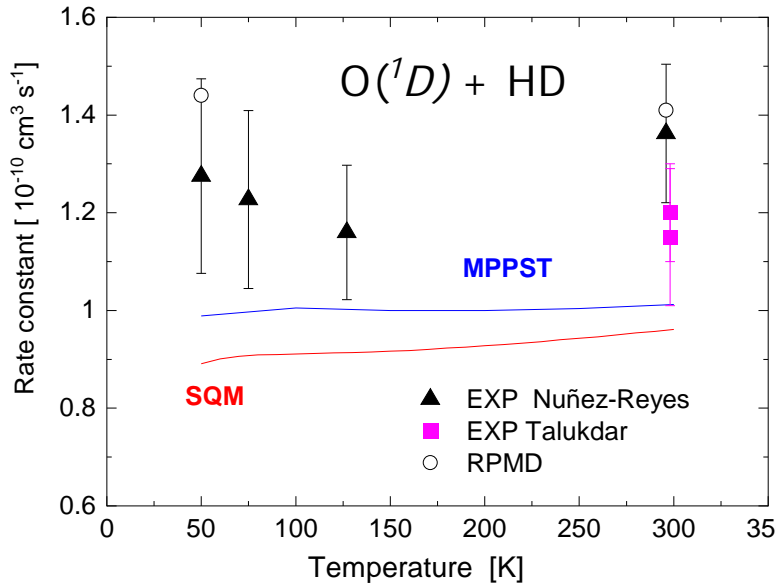


Figure 15. Rate constants for the  $O(^1D)+HD$  reaction. Experimental results from our work Nuñez-Reyes *et al.* [39] (black triangles) and Talukdar *et al.* [162] (magenta squares), are compared with theoretical results from MPPST (blue line), SQM (red line) and RPMD from our work Nuñez-Reyes *et al.* Ref. [39].

[39] and, on the other hand, at  $T = 296$  K, the RPMD estimate is in a remarkably good accord with the value reported by Hsu *et al.* [129]. In any case, results shown in Table 4 consistently suggest the preference for the H-atom production channel. One might attribute the observed higher probability for the H atom loss to a stronger O–D bond in comparison with the O–H bond once the insertion complex D–O–H is formed during the course of the reaction.

## 7. $S(^1D)+H_2$

In a remarkable effort to describe the PES characterising the  $S(^1D)+H_2 \rightarrow SH + H$  process, Zyubin *et al.* [167] computed the corresponding five lowest singlet states  $1A'$ ,  $2A'$ ,  $3A'$ ,  $1A''$  and  $2A''$  by means of *ab initio* calculations. Their results confirmed a barrierless insertion pathway along the T-shaped geometry and a collinear abstraction channel with a barrier of about 0.35 eV, which suggests a minor role of this pathway for this reaction in comparison with, for example,  $O(^1D)+H_2$ , with a noticeably smaller value for such a barrier. A similar comparative analysis with respect to  $O(^1D)+H_2$ , reveals that the effect of excited states such as  $1A''$  and  $2A'$  is less significant for the case of the  $S(^1D)+H_2$  reaction. Therefore, for not too high collision energies, the reaction is restricted to the ground state surface, which exhibits a  $H_2S$  well depth of about 3.9 eV. A first analytical fit to this ground state  $1^1A'$  PES was performed in Ref. [167] with subsequently improvements by Ho *et al.*

Table 4. Isotopic branching ratios (OD + H / OH + D) for selected values of the temperature (in K) for the O(<sup>1</sup>D)+HD reaction. Experimental results (shown in the upper part of the table) are taken directly from Refs. [39, 133, 162] and interpolated from Ref. [129]. Our theoretical rates (shown at the bottom of the table) are taken from SQM, MPPST and RPMD calculations of Ref. [39] by Nun ez-Reyes *et al.*.

$T$ (K)	50	75	127	296
Nun�ez-Reyes <i>et al.</i> [39]	1.33	1.15	1.46	1.17
Hsu <i>et al.</i> [129]	1.01	1.01	1.02	1.02
Talukdar <i>et al.</i> [162]				1.33
Tsukiyama <i>et al.</i> [133]				1.13
SQM	1.74	1.74	1.75	1.78
MPPST	1.84	1.85	1.86	1.89
RPMD	1.28			1.06

[168]. The reaction has also been the subject of investigation of the importance of electronic quenching due to the S(<sup>3</sup>P,<sup>1</sup>D)+ H<sub>2</sub> → SH + H crossing during the course of the reaction. In order to study this issue, Maiti *et al.* [169] calculated surfaces for the 1<sup>3</sup>A' and 1<sup>3</sup>A'' states. Using the result for the first singlet 1<sup>1</sup>A' given by Ho *et al.* [168], they concluded from trajectory surface-hopping calculations an important interaction between this singlet and the two aboved mentioned triplet states in the entrance channel, which leads a decrease of a factor of 2 of the corresponding S(<sup>1</sup>D)+ H<sub>2</sub> reactive cross sections [169]. However, as pointed out by Aoiz *et al.* [12], this reduction should lead to a more noticeable effect on the theoretical rate constants which would thus show less good agreement with experiment.

Excitation functions for the all possible isotopic variants were obtained at a range of larger values of  $E_c$ , between 0.026 and 0.26 eV in the pioneering experimental work by Lee and Liu [5, 170, 171]. The branching ratios between the cross sections corresponding to the SD + H-forming and the SH + D-forming product channels remained almost constant around 0.7 over the entire energy range considered in that work, a smaller value than measurements reported by Ianagaki *et al.* [172] ( $0.9 \pm 0.1$ ) and Tsukiyama *et al.* [133] ( $1.91 \pm 0.10$ ). Lee and Liu [170] also found surprising the trend followed by the corresponding cross sections of the three reactions:  $\sigma_{\text{HD}} > \sigma_{\text{D}_2} > \sigma_{\text{H}_2}$  which consequently yield an unexpected sequence for the thermal rate constants.

Angular distributions and DCSs were mapped out by means of a Doppler-selected TOF method for the S(<sup>1</sup>D) + D<sub>2</sub> reaction at a collision energy of 5.3 kcal mol<sup>-1</sup>

(0.23 eV) [171] and for the  $S(^1D) + H_2$  at 0.097 and 0.17 eV [5]. Despite some deviations with respect to PST predictions, the almost symmetric profiles observed for the distributions of this work and the possibility to understand global attributes such as the energy disposal and vibrational branching led the authors to conclude the importance of complex-forming mechanisms during the course of these reactions.

The successive refinements of the PES describing the reaction were carried out after the QCT calculations [167, 173] performed on the PES reported by Zyubin *et al.* [167] did not entirely reproduce the experimental information provided by the work of Lee and Liu [170]. In particular, the theoretical isotope H/D ratio overestimates the measured one and cross sections deviate from the experimental excitation functions in the low energy regime. Improvements introduced in the PES [168] did not lead however to noticeable changes and the theoretically calculated  $\sigma_{H_2}/\sigma_{D_2}$  and  $\sigma_{SD+H}/\sigma_{SH+D}$  ratios continued to differ from those obtained in the experiments of Ref. [170]. Similar deviations were observed in the QCT and capture model calculations performed by Bañares *et al.* [174].

The interest in the  $S(^1D)+H_2$  reaction has been renewed in recent years due to the intense work devoted to characterize this process and the isotopic variants at low energy and temperature. Thus, kinetics and CMB experiments have managed to provide detailed information on the dynamics of  $S(^1D)+H_2/D_2/HD$  reactive collisions down to temperatures as low as  $\sim 6$  K and collision energies of  $\sim 0.5$  meV [17, 175–177]. In addition to this, ICSs obtained with TIQM calculations performed on the *ab initio* ground state  $^1A'$  PES from Ref. [168] were found to describe fairly well the measured excitation functions, with the only exceptions of some deviations at the larger collision energies (beyond  $E_c \approx 0.01$  eV) seen for the case of  $S(^1D)+D_2$  [176]. In their study of the  $S(^1D)+HD$  reaction, Lara *et al.* [177] also mentioned the apparent deficiencies of the calculation to correctly describe the resonance-like oscillations seen in the corresponding measured excitation functions for the  $SH + D$  product arrangement and the branching ratio with the other product channel,  $SD+H$ .

The impressive experimental breakthrough on the title reactions has also been accompanied by a series of QM calculations to obtain reaction probabilities and ICSs. Different TDWP approaches have been applied to study the  $S(^1D)+H_2$  [178–181], the  $S(^1D)+D_2$  [182] and the  $S(^1D)+HD$  reactions [183, 184] on various PESs [168, 181, 185, 186]. Analogously, since the early work by Honvault and Launay [187] to reproduce both DCS and PTE distributions from Lee and Liu’s measurements, other TIQM calculations have been reported [17, 174–177, 188–192].

Many authors have concluded that the overall dynamics for  $S(^1D)+H_2$  correspond to an insertion mechanism involving the formation of an intermediate complex [5, 167, 188]. Such a possibility has encouraged in fact the study of the reaction in the past by means of statistical techniques. Thus, applications of the already mentioned PST [5, 51, 176, 191], a collision complex theory [193] and versions of the SQM approach [9, 42] have been reported in the literature [9, 10, 40, 41, 44, 46, 189]. DCSs obtained from QM calculations [187] and measured experimentally by Lee and Liu [5] for the  $S(^1D)+H_2$  reaction at 0.097 eV have been successfully reproduced by statistical means [9, 10, 46]. The same good agreement [10, 46] with the corresponding rovibrational cross sections reported by Honvault and Launay [187] and with the experimental

PTE distributions [10] at the same energy from Ref. [5] was achieved with statistical predictions. Besides the study by Lin and Guo [46], efforts to reproduce some of the dynamical features measured for the  $S(^1D)+D_2$  reaction at 0.23 eV [171] such as the DCS and the PTE distribution [10] have also revealed the importance of the complex forming mechanism for this reactive collision. Moreover, both  $S(^1D)+H_2$  and  $S(^1D)+D_2$  reactions have been investigated [194, 195] via the multi-PES statistical theory developed by Alexander *et al.* [150] as an extension of the single-surface SQM of Ref. [9]. Examples of studies employing statistical methods in the low energy and temperature regimes are the application of a semi-classical capture model [51, 176] and MPPST to study the  $S(^1D)+H_2/D_2$  reactions [191], and the approach by Grozdanov and McCarroll [196] applied to the  $S(^1D)+HD$  reaction.

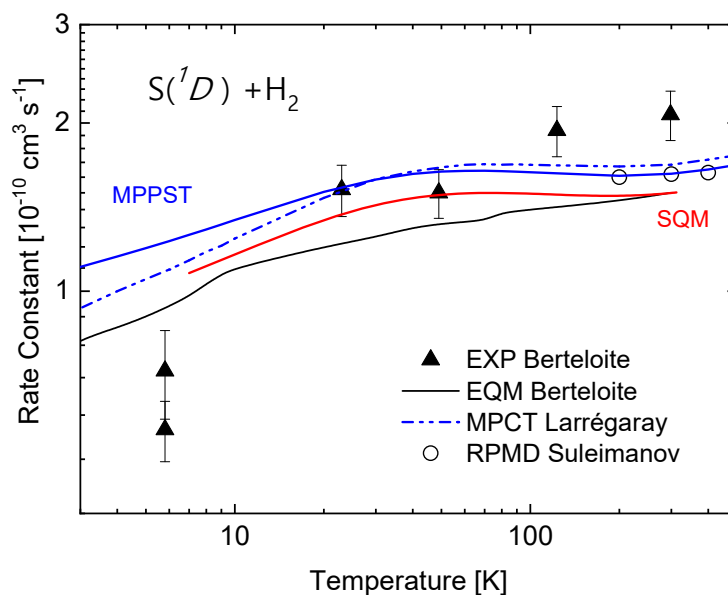


Figure 16. Rate constants for the  $S(^1D)+H_2$  reaction. Experimental results are from Berteloite *et al.* [17] (black triangles) and are compared with our MPPST (solid blue line) and SQM (red line) from González-Lezana *et al.* [41], RPMD (open black circles) from Suleimanov *et al.* [66], EQM (black line) from Berteloite *et al.* [17] and MPCT (blue dashed line) from Larrégaray *et al.* [51]

Despite the interest on the removal mechanisms for  $S(^1D)$  shown in the past [197, 198], the kinetics of the  $S(^1D)+H_2$  reaction has been investigated only on a few occasions. Thus, apart from the determination of the rate constant at  $T = 300$  K [199] and a resonance-enhanced photoionization study to measure the branching ratio for quenching of  $S(^1D)$  in collision with different gases performed by Black [200], no previous record of kinetics investigations can be found in the literature before those reported in Ref. [17]. In that recent work, the kinetics experiments approached the cold regime ( $T < 1$  K) and values of the rate constant for the  $S(^1D)+H_2$  reaction

were obtained from room temperature (298 K) down to 5.8 K. The results of these measurements are shown in Figure 16 alongside a series of theoretical predictions from different calculations: EQM from Ref. [17], RMPD by Suleimanov [66], the MPCT approach by Larrégaray *et al* [51] and the SQM and MPPST results from Ref. [41]. The comparison between experiment and theory reveals that the statistical techniques certainly provide a good description of the measured rate constant for the above mentioned low temperature range. In particular, the three alternatives, that is, SQM, MPPST and MPCT, are in somewhat better agreement with the experimental values than the TIQM results by Berteloite *et al.* [17] with the only exception of  $k(T = 5.8 \text{ K})$ .

## 8. Conclusions

Recent experimental investigations have provided interesting information regarding the kinetics of the reactions between molecular hydrogen and the electronically excited atoms C(<sup>1</sup>D), N(<sup>2</sup>D), O(<sup>1</sup>D) and S(<sup>1</sup>D). Rate constants over a range of temperature between 10 K and 300 K are now available. The comparison with theoretical results reveals the good performance of the statistical and capture theory techniques, thus supporting the essentially complex-forming nature of these reactions, as expected from the existence of relatively deep potential wells in the intermediate region between reactants and products. In some cases however, the contribution from excited electronic states is required for a complete agreement with the measured rate constants.

## 9. Acknowledgments

T.G.L. thanks MINECO/AEI/FEDER, UE, Spain for support with Grant FIS2017-83157-P. K.M.H. acknowledges support from the French program “Physique et Chimie du Milieu Interstellaire” (PCMI) of the CNRS/INSU with the INC/INP co-funded by the CEA and CNES as well as funding from the “Program National de Planétologie” (PNP) of the CNRS/INSU.

## References

- [1] X. Liu, J. J. Lin, S. Harich, G. C. Schatz, and X. Yang, *Science* **289** (5484), 1536–1538 (2000). <<https://doi.org/10.1126/science.289.5484.1536>>.
- [2] X. Yang, *Phys. Chem. Chem. Phys.* **13**, 8112–8121 (2011). <<http://dx.doi.org/10.1039/C1CP00005E>>.
- [3] P. Casavecchia, N. Balucani, and G. G. Volpi, *Annu. Rev. Phys. Chem.* **50** (1), 347–376 (1999). <<https://doi.org/10.1146/annurev.physchem.50.1.347>>, PMID: 15012416.
- [4] K. Liu, *Annu. Rev. Phys. Chem.* **52** (1), 139–164 (2001). <<https://doi.org/10.1146/annurev.physchem.52.1.139>>, PMID: 11326062.
- [5] S. H. Lee and K. Liu, *Appl. Phys. B* **71**, 627 (2000). <<https://doi.org/10.1007/s003400000386>>.
- [6] N. Balucani, L. Cartechini, G. Capozza, E. Segoloni, P. Casavecchia, G. G. Volpi, F. J. Aoiz, L. Bañares, P. Honvault, and J. M. Launay, *Phys. Rev. Lett.* **89** (1), 013201 (2002). <<https://doi.org/10.1103/PhysRevLett.89.013201>>.
- [7] N. Balucani, G. Capozza, L. Cartechini, A. Bergeat, R. Bobbenkamp, P. Casavecchia, F. J. Aoiz, L. Bañares, P. Honvault, B. Bussery-Honvault, and J. Launay, *Phys. Chem. Chem. Phys.* **6** (21), 4957–4967 (2004). <<https://doi.org/10.1039/b409327e>>.
- [8] N. Balucani, G. Capozza, E. Segoloni, A. Russo, R. Bobbenkamp, P. Casavecchia, T. González-Lezana, E. J. Rackham, L. Bañares, and F. J. Aoiz, *J. Chem. Phys.* **122**, 234309 (2005). <<https://doi.org/10.1063/1.1930831>>.
- [9] E. J. Rackham, T. González-Lezana, and D. E. Manolopoulos, *J. Chem. Phys.* **119**, 12895 (2003). <<https://doi.org/10.1063/1.1628218>>.
- [10] T. González-Lezana, *Int. Rev. Phys. Chem.* **26**, 29 (2007). <<https://doi.org/10.1080/03081070600933476>>.
- [11] H. Guo, *Int. Rev. Phys. Chem.* **31** (1), 1–68 (2012). <<https://doi.org/10.1080/0144235X.2011.649999>>.
- [12] F. J. Aoiz, L. Bañares, and V. J. Herrero, *J. Phys. Chem. A* **110** (46), 12546–12565 (2006). <<https://doi.org/10.1021/jp0063815o>>.
- [13] M. Hawley, T. Mazely, L. Randeniya, R. Smith, X. Zeng, and M. Smith, *Int. J. Mass Spectrom. Ion Processes* **97** (1), 55–86 (1990). <<https://www.sciencedirect.com/science/article/pii/0168117690850409>>.
- [14] B. R. Rowe, G. Dupeyrat, J. B. Marquette, and P. Gaucherel, *J. Chem. Phys.* **80** (10), 4915–4921 (1984). <<https://doi.org/10.1063/1.446513>>.
- [15] I. R. Sims, I. W. M. Smith, P. Bocherel, A. Defrance, D. Travers, and B. R. Rowe, *J. Chem. Soc., Faraday Trans.* **90**, 1473–1478 (1994). <<http://dx.doi.org/10.1039/FT9949001473>>.
- [16] A. Potapov, A. Canosa, E. Jiménez, and B. Rowe, *Angew. Chem. Int. Ed.* **56** (30), 8618–8640 (2017). <<https://onlinelibrary.wiley.com/doi/abs/10.1002/anie.201611240>>.
- [17] C. Berteloite, M. Lara, A. Bergeat, S. D. Le Picard, F. Dayou, K. M. Hickson, A. Canosa, C. Naulin, J. M. Launay, I. R. Sims, and M. Costes, *Phys. Rev. Lett.* **105**, 203201 (2010). <<https://doi.org/10.1103/PhysRevLett.105.203201>>.
- [18] R. Grondin, J. C. Loison, and K. M. Hickson, *J. Phys. Chem. A* **120** (27), 4838–4844 (2016). <<https://doi.org/10.1021/acs.jpca.5b12358>>, PMID: 26814664.
- [19] A. Bergeat, T. Calvo, G. Dorthé, and J. Loison, *Chem. Phys. Lett.* **308** (1), 7–12 (1999). <<https://www.sciencedirect.com/science/article/pii/S0009261499005862>>.
- [20] R. J. Shannon, C. Cossou, J. C. Loison, P. Caubet, N. Balucani, P. W. Seakins, V. Wakelam, and K. M. Hickson, *RSC Adv.* **4**, 26342–26353 (2014). <<http://dx.doi.org/10.1039/C4RA03036B>>.
- [21] D. Nuñez Reyes and K. M. Hickson, *Phys. Chem. Chem. Phys.* **20**, 17442–17447 (2018). <<http://dx.doi.org/10.1039/C8CP02851F>>.
- [22] M. Lara, C. Berteloite, M. Paniagua, F. Dayou, S. D. Le Picard, and J. M. Launay, *Phys. Chem. Chem. Phys.* **19**, 28555–28571 (2017). <<http://dx.doi.org/10.1039/C7CP05279K>>.
- [23] R. Hilbig and R. Wallenstein, *IEEE J. Quant. Electron.* **17** (8), 1566–1573 (1981).

- [24] K. M. Hickson, J. C. Loison, H. Guo, and Y. V. Suleimanov, *J. Phys. Chem. Lett.* **6** (21), 4194–4199 (2015). <<https://doi.org/10.1021/acs.jpcllett.5b02060>>.
- [25] D. Husain and L. J. Kirsch, *Trans. Faraday Soc.* **67**, 2886–2895 (1971). <<http://dx.doi.org/10.1039/TF9716702886>>.
- [26] K. M. Hickson and Y. V. Suleimanov, *Phys. Chem. Chem. Phys.* **19**, 480–486 (2017). <<https://doi.org/10.1039/C6CP07381F>>.
- [27] D. Nuñez Reyes and K. M. Hickson, *J. Phys. Chem. A* **122** (20), 4696–4703 (2018). <<https://doi.org/10.1021/acs.jpca.8b02267>>, PMID: 29715024.
- [28] E. Carmona-Novillo, T. González-Lezana, O. Roncero, P. Honvault, J. M. Launay, N. Bulut, F. J. Aoiz, L. Bañares, A. Trottier, and E. Wrede, *J. Chem. Phys.* **128**, 014304 (2008). <<https://doi.org/10.1063/1.2812555>>.
- [29] F. Dayou, P. Larrégaray, L. Bonnet, J. C. Rayez, P. N. Arenas, and T. González-Lezana, *J. Chem. Phys.* **128**, 174307 (2008). <<https://doi.org/10.1063/1.2913156>>.
- [30] P. Bargueño, T. González-Lezana, P. Larrégaray, L. Bonnet, J.-C. Rayez, M. Hankel, S. C. Smith and A. J. H. M. Meijer, *J. Chem. Phys.* **128**, 244308 (2008). <<https://doi.org/10.1063/1.2944246>>.
- [31] A. Rivero-Santamaría, M. L. González-Martínez, T. González-Lezana, J. Rubayo-Soneira, L. Bonnet, and P. Larrégaray, *Phys. Chem. Chem. Phys.* **13**, 8136–8139 (2011). <<https://doi.org/10.1039/c0cp02662j>>.
- [32] T. González-Lezana and P. Honvault, *Int. Rev. Phys. Chem.* **33** (3), 371–395 (2014). <<https://doi.org/10.1080/0144235X.2014.943470>>.
- [33] D. Nuñez Reyes, K. M. Hickson, P. Larrégaray, L. Bonnet, T. González-Lezana, and Y. V. Suleimanov, *Phys. Chem. Chem. Phys.* **20**, 4404–4414 (2018). <<https://doi.org/10.1039/C7CP07843A>>.
- [34] T. González-Lezana, P. Larrégaray, L. Bonnet, Y. Wu, and W. Bian, *J. Chem. Phys.* **148** (23), 234305 (2018). <<https://doi.org/10.1063/1.5026454>>.
- [35] P. Larrégaray, L. Bonnet, and J. C. Rayez, *J. Chem. Phys.* **127** (8), 084308 (2007). <<https://doi.org/10.1063/1.2768959>>.
- [36] P. Larrégaray, L. Bonnet, and J. C. Rayez, *J. Phys. Chem. A* **110** (4), 1552–1560 (2006). <<https://doi.org/10.1021/jp053822x>>.
- [37] L. Bonnet, P. Larrégaray, and J. C. Rayez, *Phys. Chem. Chem. Phys.* **25** (9), 3228–3240 (2007). <<https://doi.org/10.1039/B700906B>>.
- [38] D. Nuñez-Reyes, C. Bray, K. M. Hickson, P. Larrégaray, L. Bonnet, and T. González-Lezana, *Phys. Chem. Chem. Phys.* **22**, 23609–23617 (2020). <<http://dx.doi.org/10.1039/D0CP03971C>>.
- [39] D. Nuñez Reyes, K. M. Hickson, P. Larrégaray, L. Bonnet, T. González-Lezana, S. Bhowmick, and Y. V. Suleimanov, *J. Phys. Chem. A* **123** (38), 8089–8098 (2019). <<https://doi.org/10.1021/acs.jpca.9b06133>>.
- [40] T. González-Lezana, P. Larrégaray, and L. Bonnet, *Chem. Phys. Lett.* **763**, 138228 (2021). <<http://www.sciencedirect.com/science/article/pii/S0009261420311283>>.
- [41] T. González-Lezana, P. Larrégaray, and L. Bonnet, QUARKS: Braz. Electron. J. Phys. Chem. Mat. Sci. **3**, 9–16 (2020). <<https://doi.org/10.34019/2674-9688.2020.v3.30914>>.
- [42] E. J. Rackham, F. Huarte-Larrañaga, and D. E. Manolopoulos, *Chem. Phys. Lett.* **343** (3–4), 356 – 364 (2001). <[http://dx.doi.org/10.1016/S0009-2614\(01\)00707-2](http://dx.doi.org/10.1016/S0009-2614(01)00707-2)>.
- [43] F. J. Aoiz, T. González-Lezana, and V. Sáez Rábanos, *J. Chem. Phys.* **127**, 174109 (2007). <<https://doi.org/10.1063/1.2774982>>.
- [44] F. J. Aoiz, T. González-Lezana, and V. S. Rábanos, *J. Chem. Phys.* **129**, 094305 (2008). <<https://doi.org/10.1063/1.2969812>>.
- [45] F. J. Aoiz, V. Sáez Rábanos, T. González-Lezana, and D. E. Manolopoulos, *J. Chem. Phys.* **126**, 161101 (2007). <<https://doi.org/10.1063/1.2723067>>.
- [46] S. Y. Lin and H. Guo, *J. Chem. Phys.* **122** (7), 074304 (2005). <<http://dx.doi.org/10.1063/1.1851500>>.
- [47] P. Pechukas, J. C. Light, and C. Rankin, *J. Chem. Phys.* **44**, 794 (1966). <<https://doi.org/10.1063/1.1726760>>.
- [48] E. E. Nikitin, *Theory of elementary atomic and molecular processes in gases* (, ,

- 1974).
- [49] L. Bonnet and J. C. Rayez, *Phys. Chem. Chem. Phys.* **1**, 2383–2400 (1999). <<https://doi.org/10.1021/jp053822x>>.
- [50] M. L. González-Martínez, O. Dulieu, P. Larrégaray, and L. Bonnet, *Phys. Rev. A* **90**, 052716 (2014). <<https://doi.org/10.1103/PhysRevA.90.052716>>.
- [51] P. Larrégaray and L. Bonnet, *Comp. Theor. Chem.* **990** (Supplement C), 18 – 22 (2012). <<https://doi.org/10.1016/j.comptc.2012.02.012>>.
- [52] J. Davidsson and G. Nyman, *Chem. Phys.* **125**, 171–183 (1988). <[https://doi.org/10.1016/0301-0104\(88\)87073-3](https://doi.org/10.1016/0301-0104(88)87073-3)>.
- [53] T. P. Grozdanov and R. McCarroll, *J. Phys. Chem. A* **115**, 6872–6877 (2011). <<https://doi.org/10.1021/jp1115228>>.
- [54] P. Larrégaray and L. Bonnet, *J. Chem. Phys.* **143**, 144113 (2015). <<https://doi.org/10.1063/1.4933009>>.
- [55] L. Bonnet and P. Larrégaray, *J. Chem. Phys.* **152**, 08417 (2020). <<https://doi.org/10.1063/1.5139207>>.
- [56] B. Bussery-Honvault, P. Honvault, and J. M. Launay, *J. Chem. Phys.* **115** (23), 10701–10708 (2001). <<https://doi.org/10.1063/1.1417501>>.
- [57] L. Bañares, F. Aoiz, S. A. Vázquez, T. S. Ho, and H. Rabitz, *Chem. Phys. Lett.* **374** (3), 243 – 251 (2003). <<http://www.sciencedirect.com/science/article/pii/S0009261403007152>>.
- [58] X. Liu, W. Bian, X. Zhao, and X. Tao, *J. Chem. Phys.* **125** (7), 074306 (2006). <<https://doi.org/10.1063/1.2263769>>.
- [59] S. Joseph, P. J. S. B. Caridade, and A. J. C. Varandas, *J. Phys. Chem. A* **115** (27), 7882–7890 (2011). <<https://doi.org/10.1021/jp2032912>>.
- [60] Y. Wu, C. Zhang, J. Cao, and W. Bian, *J. Phys. Chem. A* **118** (24), 4235–4242 (2014). <<https://doi.org/10.1021/jp504411j>>.
- [61] C. Zhang, M. Fu, Z. Shen, H. Ma, and W. Bian, *J. Chem. Phys.* **140** (23), 234301 (2014). <<https://doi.org/10.1063/1.4881896>>.
- [62] Z. Sun, C. Zhang, S. Lin, Y. Zheng, Q. Meng, and W. Bian, *J. Chem. Phys.* **139** (1), 014306 (2013). <<https://doi.org/10.1063/1.4811844>>.
- [63] P. Defazio, C. Petrongolo, B. Bussery-Honvault, and P. Honvault, *J. Chem. Phys.* **131** (11), 114303 (2009). <<https://doi.org/10.1063/1.3226573>>.
- [64] P. Defazio, B. Bussery-Honvault, P. Honvault, and C. Petrongolo, *J. Chem. Phys.* **135** (11), 114308 (2011). <<https://doi.org/10.1063/1.3636083>>.
- [65] K. Sato, N. Ishida, T. Kurakata, A. Iwasaki, and S. Tsunashima, *Chem. Phys.* **237** (1), 195 – 204 (1998). <<http://www.sciencedirect.com/science/article/pii/S0301010498001839>>.
- [66] Y. V. Suleimanov, W. J. Kong, H. Guo, and W. H. Green, *J. Chem. Phys.* **141** (24), 244103 (2014). <<https://doi.org/10.1063/1.4904080>>.
- [67] B. Bussery-Honvault, J. Julien, P. Honvault, and J. M. Launay, *Phys. Chem. Chem. Phys.* **7**, 1476–1481 (2005). <<https://doi.org/10.1039/B419000A>>.
- [68] Z. Shen, H. Ma, C. Zhang, M. Fu, Y. Wu, W. Bian, and J. Cao, *Nature Comm.* **8**, 14094 (2017). <<https://doi.org/10.1038/ncomms14094>>.
- [69] Y. Wu, J. Cao, H. Ma, C. Zhang, W. Bian, D. Nunez-Reyes, and K. M. Hickson, *Sci. Adv.* **5** (4) (2019). <<https://doi.org/10.1126/sciadv.aaw0446>>.
- [70] W. Fisher, T. Carrington, C. Sadowski, and C. Dugan, *Chem. Phys.* **97** (2), 433 – 448 (1985). <<http://www.sciencedirect.com/science/article/pii/0301010485870518>>.
- [71] D. Husain and L. Kirsch, *Chem. Phys. Lett.* **9** (5), 412 – 415 (1971). <<http://www.sciencedirect.com/science/article/pii/0009261471802555>>.
- [72] P. Defazio, P. Gamallo, M. González, S. Akpınar, B. Bussery-Honvault, P. Honvault, and C. Petrongolo, *J. Chem. Phys.* **132** (10), 104306 (2010). <<https://doi.org/10.1063/1.3342061>>.
- [73] N. Balucani, P. Casavecchia, F. Aoiz, L. Bañares, J. M. Launay, B. Bussery-Honvault, and P. Honvault, *Mol. Phys.* **108** (3-4), 373–380 (2010). <<https://doi.org/10.1080/00268970903476696>>.
- [74] G. M. Jursich and J. R. Wiesenfeld, *Chem. Phys. Lett.* **110** (1), 14 – 19 (1984).

- <<http://www.sciencedirect.com/science/article/pii/0009261484801372>>.
- [75] L. B. Harding, R. Guadagnini, and G. C. Schatz, *J. Phys. Chem.* **97** (21), 5472–5481 (1993). <<https://doi.org/10.1021/j100123a005>>.
- [76] A. Bergeat, L. Cartechini, N. Balucani, G. Capozza, L. Phillips, P. Casavecchia, G. Volpi, L. Bonnet, and J. C. Rayez, *Chem. Phys. Lett.* **327** (3), 197 – 202 (2000). <<http://www.sciencedirect.com/science/article/pii/S0009261400008708>>.
- [77] S. Lin and H. Guo, *J. Chem. Phys.* **121** (3), 1285–1292 (2004). <<https://doi.org/10.1063/1.1764502>>.
- [78] S. Lin and H. Guo, *J. Phys. Chem. A* **108** (12), 2141–2148 (2004). <<https://doi.org/10.1021/jp031184h>>.
- [79] L. Bañares, F. Aoiz, P. Honvault, B. Bussery-Honvault, and J. Launay, *J. Chem. Phys.* **118** (2), 565 (2003). <<https://doi.org/10.1063/1.1527014>>.
- [80] Z. Shen, J. Cao, and W. Bian, *J. Chem. Phys.* **142** (16), 164309 (2015). <<https://doi.org/10.1063/1.4919406>>.
- [81] S. Lin and H. Guo, *J. Chem. Phys.* **120** (21), 9907–9910 (2004). <<https://doi.org/10.1063/1.1756584>>.
- [82] S. Lin and H. Guo, *J. Phys. Chem. A* **108** (46), 10066–10071 (2004). <<https://doi.org/10.1021/jp046039y>>.
- [83] L. Bonnet, P. Larrégaray, J. C. Rayez, and T. González-Lezana, *Phys. Chem. Chem. Phys.* **8**, 3951 (2006). <<https://doi.org/10.1039/b608811b>>.
- [84] Hébrard, E., Dobrijevic, M., Loison, J. C., Bergeat, A., Hickson, K. M., and Caralp, F., *A&A* **552**, A132 (2013). <<https://doi.org/10.1051/0004-6361/201220686>>.
- [85] T. Suzuki, Y. Shihira, T. Sato, H. Umemoto, and S. Tsunashima, *J. Chem. Soc., Faraday Trans.* **89**, 995–999 (1993). <<https://doi.org/10.1039/FT9938900995>>.
- [86] P. Defazio and C. Petrongolo, *J. Chem. Phys.* **125** (6), 064308 (2006). <<https://doi.org/10.1063/1.2229212>>.
- [87] H. Kobayashi, T. Takayanagi, K. Yokoyama, T. Sato, and S. Tsunashima, *J. Chem. Soc., Faraday Trans.* **91**, 3771–3777 (1995). <<https://doi.org/10.1039/FT9959103771>>.
- [88] T. Takayanagi, H. Kobayashi, and S. Tsunashima, *J. Chem. Soc., Faraday Trans.* **92**, 1311–1314 (1996). <<https://doi.org/10.1039/FT9969201311>>.
- [89] H. Kobayashi, T. Takayanagi, and S. Tsunashima, *Chemical Physics Letters* **277** (1), 20 – 26 (1997). <[https://doi.org/10.1016/S0009-2614\(97\)00892-0](https://doi.org/10.1016/S0009-2614(97)00892-0)>.
- [90] L. A. Pederson, G. C. Schatz, T. S. Ho, T. Hollebeek, H. Rabitz, L. B. Harding, and G. Lendvay, *J. Chem. Phys.* **110** (18), 9091–9100 (1999). <<https://doi.org/10.1063/1.478830>>.
- [91] J. A. Dodd, S. J. Lipson, D. J. Flanagan, W. A. M. Blumberg, J. C. Person, and B. D. Green, *J. Chem. Phys.* **94** (6), 4301–4310 (1991). <<https://doi.org/10.1063/1.460616>>.
- [92] H. Umemoto and K. Matsumoto, *The Journal of Chemical Physics* **104** (23), 9640–9643 (1996). <<https://doi.org/10.1063/1.471716>>.
- [93] H. Umemoto, T. Asai, and Y. Kimura, *J. Chem. Phys.* **106** (12), 4985–4991 (1997). <<https://doi.org/10.1063/1.473546>>.
- [94] H. Umemoto, *Chem. Phys. Lett.* **292** (4), 594 – 600 (1998).
- [95] P. Honvault and J. M. Launay, *J. Chem. Phys.* **111**, 6665–6667 (1999). <<http://link.aip.org/link/?JCP/111/6665/1>>.
- [96] H. Umemoto, N. Terada, and K. Tanaka, *The Journal of Chemical Physics* **112** (13), 5762–5766 (2000). <<https://doi.org/10.1063/1.481151>>.
- [97] M. Alagia, N. Balucani, L. Cartechini, P. Casavecchia, G. G. Volpi, L. A. Pederson, G. C. Schatz, G. Lendvay, L. B. Harding, T. Hollebeek, T. S. Ho, and H. Rabitz, *J. Chem. Phys.* **110** (18), 8857–8860 (1999). <<https://doi.org/10.1063/1.478806>>.
- [98] N. Balucani, M. Alagia, L. Cartechini, P. Casavecchia, G. G. Volpi, L. A. Pederson, and G. C. Schatz, *J. Phys. Chem. A* **105** (11), 2414–2422 (2001). <<https://doi.org/10.1021/jp0036238>>.
- [99] A. Kowalski, B. Pranszke, S. Werbowy, and C. Ottinger, *Chem. Phys. Lett.* **389** (1), 218 – 224 (2004). <<https://doi.org/10.1016/j.cplett.2004.03.102>>.

- [100] S. Y. Lin, L. Bañares, and H. Guo, *J. Phys. Chem. A* **111** (12), 2376–2384 (2007). <<https://doi.org/10.1021/jp0682715>>.
- [101] S. Y. Lin, H. Guo, B. Jiang, S. Zhou, and D. Xie, *J. Phys. Chem. A* **114** (36), 9655–9661 (2010), PMID: 20394452.
- [102] Z. Zhu, H. Wang, X. Wang, and Y. Shi, *Molecular Physics* **116** (9), 1108–1117 (2018). <<https://doi.org/10.1080/00268976.2017.1398355>>.
- [103] N. Balucani, P. Casavecchia, L. Bañares, F. J. Aoiz, T. González-Lezana, P. Honvault, and J. M. Launay, *J. Phys. Chem. A* **110**, 817 (2006). <<https://doi.org/10.1021/jp054928v>>.
- [104] G. Black, T. G. Slanger, G. A. St. John, and R. A. Young, *J. Chem. Phys.* **51** (1), 116–121 (1969). <<https://doi.org/10.1063/1.1671694>>.
- [105] D. Husain, L. J. Kirsch, and J. R. Wiesenfeld, *Faraday Discuss. Chem. Soc.* **53**, 201–210 (1972). <<https://doi.org/10.1039/DC9725300201>>.
- [106] D. Husain, S. K. Mitra, and A. N. Young, *J. Chem. Soc., Faraday Trans. 2* **70**, 1721–1731 (1974). <<https://doi.org/10.1039/F29747001721>>.
- [107] G. Black, R. L. Sharpless, T. G. Slanger, and D. C. Lorents, *J. Chem. Phys.* **62** (11), 4266–4273 (1975). <<https://doi.org/10.1063/1.430347>>.
- [108] B. Fell, I. V. Rivas, and D. L. McFadden, *J. Phys. Chem.* **85** (3), 224–228 (1981).
- [109] P. D. Whitefield and F. E. Hovis, *Chem. Phys. Lett.* **135** (4), 454 – 458 (1987). <[https://doi.org/10.1016/0009-2614\(87\)85189-8](https://doi.org/10.1016/0009-2614(87)85189-8)>.
- [110] L. G. Piper, M. E. Donahue, and W. T. Rawlins, *J. Phys. Chem.* **91** (14), 3883–3888 (1987). <<https://doi.org/10.1021/j100298a030>>.
- [111] H. Umemoto, N. Hachiya, E. Matsunaga, A. Suda, and M. Kawasaki, *Chem. Phys. Lett.* **296** (1), 203 – 207 (1998). <[https://doi.org/10.1016/S0009-2614\(98\)01006-9](https://doi.org/10.1016/S0009-2614(98)01006-9)>.
- [112] T. S. Ho, H. Rabitz, F. J. Aoiz, L. Bañares, S. A. Vázquez, and L. B. Harding, *J. Chem. Phys.* **119** (6), 3063–3070 (2003). <<https://doi.org/10.1063/1.1588632>>.
- [113] J. T. Herron, *J. Phys. Chem. Ref. Data* **28** (5), 1453–1483 (1999). <<https://doi.org/10.1063/1.556043>>.
- [114] J. A. Schmidt, M. S. Johnson, and R. Schinke, *Proc. Natl. Acad. Sci.* **110** (44), 17691–17696 (2013). <<https://www.pnas.org/content/110/44/17691>>.
- [115] H. Nair, M. Allen, A. Anbar, Y. Yung, and R. Clancy, *Icarus* **111** (1), 124–150 (1994). <<https://doi.org/10.1006/icar.1994.1137>>.
- [116] K. M. Hickson and Y. V. Suleimanov, *J. Phys. Chem. A* **121** (9), 1916–1923 (2017). <<https://doi.org/10.1021/acs.jpca.7b00722>>, PMID: 28207257.
- [117] S. Vranckx, J. Peeters, and S. Carl, *Phys. Chem. Chem. Phys.* **12**, 9213–9221 (2010). <<http://dx.doi.org/10.1039/B923959F>>.
- [118] M. A. Blitz, T. J. Dillon, D. E. Heard, M. J. Pilling, and I. D. Trought, *Phys. Chem. Chem. Phys.* **6**, 2162–2171 (2004). <<http://dx.doi.org/10.1039/B400283K>>.
- [119] J. A. Davidson, H. I. Schiff, G. E. Streit, J. R. McAfee, A. L. Schmeltekopf, and C. J. Howard, *J. Chem. Phys.* **67** (11), 5021–5025 (1977). <<https://doi.org/10.1063/1.434724>>.
- [120] S. Y. Lin and H. Guo, *J. Phys. Chem. A* **113** (16), 4285–4293 (2009). <<https://doi.org/10.1021/jp810948k>>.
- [121] Y. Li, Y. V. Suleimanov, and H. Guo, *J. Phys. Chem. Lett.* **5** (4), 700–705 (2014). <<https://doi.org/10.1021/jz500062q>>, PMID: 26270840.
- [122] T. Ho, T. Hollebeek, H. Rabitz, L. B. Harding, and G. C. Schatz, *J. Chem. Phys.* **105** (23), 10472–10486 (1996). <<https://doi.org/10.1063/1.472977>>.
- [123] A. J. Dobbyn and P. J. Knowles, *Mol. Phys.* **91** (6), 1107–1124 (1997). <<https://doi.org/10.1080/002689797170842>>.
- [124] Y. T. Hsu, K. Liu, L. A. Pederson, and G. C. Schatz, *J. Chem. Phys.* **111** (17), 7921–7930 (1999).
- [125] M. Alagia, N. Balucani, L. Cartechini, P. Casavecchia, E. H. van Kleef, G. G. Volpi, P. J. Kuntz, and J. J. Sloan, *J. Chem. Phys.* **108** (16), 6698–6708 (1998). <<https://doi.org/10.1063/1.476085>>.
- [126] T. Peng, D. H. Zhang, J. Z. Zhang, and R. Schinke, *Chem. Phys. Lett.* **248** (1), 37–42 (1996). <<https://www.sciencedirect.com/science/article/pii/0009261495012850>>.

- [127] A. Alexander, F. Aoiz, M. Brouard, and J. Simons, *Chem. Phys. Lett.* **256** (6), 561–568 (1996). <<https://www.sciencedirect.com/science/article/pii/0009261496005064>>.
- [128] D. Che and K. Liu, *J. Chem. Phys.* **103** (12), 5164–5167 (1995). <<https://doi.org/10.1063/1.470606>>.
- [129] Y. T. Hsu, J. H. Wang, and K. Liu, *J. Chem. Phys.* **107** (7), 2351–2356 (1997).
- [130] P. Hermine, Y. Hsu, and K. Liu, *Phys. Chem. Chem. Phys.* **2**, 581–587 (2000). <<http://dx.doi.org/10.1039/A907906H>>.
- [131] G. C. Schatz, A. Papaioannou, L. A. Pederson, L. B. Harding, T. Hollebeek, T. S. Ho, and H. Rabitz, *J. Chem. Phys.* **107** (7), 2340–2350 (1997). <<https://doi.org/10.1063/1.474614>>.
- [132] R. Buss, P. Casavecchia, T. Hirooka, S. Sibener, and Y. Lee, *Chem. Phys. Lett.* **82** (3), 386–391 (1981). <<https://www.sciencedirect.com/science/article/pii/0009261481854036>>.
- [133] K. Tsukiyama, B. Katz, and R. Bersohn, *J. Chem. Phys.* **83** (6), 2889–2893 (1985). <<https://doi.org/10.1063/1.449241>>.
- [134] J. E. Butler, G. M. Jursich, I. A. Watson, and J. R. Wiesenfeld, *J. Chem. Phys.* **84** (10), 5365–5377 (1986). <<https://doi.org/10.1063/1.449947>>.
- [135] Y. Matsumi, K. Tonokura, M. Kawasaki, and H. L. Kim, *J. Phys. Chem.* **96** (26), 10622–10626 (1992). <<https://doi.org/10.1021/j100205a012>>.
- [136] T. Laurent, P. Naik, H. R. Volpp, J. Wolfrum, T. Arusi-Parpar, I. Bar, and S. Rosenwaks, *Chem. Phys. Lett.* **236** (3), 343–349 (1995). <[https://doi.org/10.1016/S0082-0784\(96\)80251-7](https://doi.org/10.1016/S0082-0784(96)80251-7)>.
- [137] Y. T. Hsu and K. Liu, *J. Chem. Phys.* **107** (5), 1664–1667 (1997). <<https://doi.org/10.1063/1.474518>>.
- [138] Y. T. Hsu, K. Liu, L. A. Pederson, and G. C. Schatz, *J. Chem. Phys.* **111** (17), 7931–7944 (1999). <<https://doi.org/10.1063/1.480128>>.
- [139] X. Liu, C. C. Wang, S. A. Harich, and X. Yang, *Phys. Rev. Lett.* **89**, 133201 (2002). <<https://link.aps.org/doi/10.1103/PhysRevLett.89.133201>>.
- [140] F. Aoiz, L. Bañares, J. Castillo, V. Herrero, B. Martinez-Haya, P. Honvault, J. Launay, X. Liu, J. Lin, S. Harich, C. Wang, and X. Yang, *J. Chem. Phys.* **116** (24), 10692–10703 (2002). <<https://doi.org/10.1063/1.1478693>>.
- [141] S. K. Gray, G. G. Balint-Kurti, G. C. Schatz, J. J. Lin, X. Liu, S. Harich, and X. Yang, *J. Chem. Phys.* **113** (17), 7330–7344 (2000). <<https://doi.org/10.1063/1.1313785>>.
- [142] X. Liu, J. J. Lin, S. A. Harich, and X. Yang, *J. Chem. Phys.* **113** (4), 1325–1328 (2000). <<https://doi.org/10.1063/1.481923>>.
- [143] N. Balucani, P. Casavecchia, F. J. Aoiz, L. Banares, J. F. Castillo, and V. J. Herrero, *Mol. Phys.* **103** (13), 1703–1714 (2005). <<https://doi.org/10.1080/149920500058077>>.
- [144] S. Kauczok, C. Maul, A. I. Chichinin, and K. H. Gericke, *J. Chem. Phys.* **132** (24), 244308 (2010). <<https://doi.org/10.1063/1.3427534>>.
- [145] X. Liu, J. J. Lin, S. A. Harich, and X. Yang, *Phys. Rev. Lett.* **86**, 408–411 (2001). <<https://link.aps.org/doi/10.1103/PhysRevLett.86.408>>.
- [146] Y. Liu, Y. Gao, D. Shi, and J. Sun, *Chem. Phys.* **364** (1), 46–50 (2009). <<https://doi.org/10.1016/j.chemphys.2009.08.010>>.
- [147] D. Kuang, T. Chen, W. Zhang, N. Zhao, and D. Wang, *Bull. Korean Chem. Soc.* **31** (10), 2841–2848 (2010). <<https://doi.org/10.5012/BKCS.2010.31.10.2841>>.
- [148] S. Y. Lin and H. Guo, *J. Chem. Phys.* **129** (12), 124311 (2008). <<https://doi.org/10.1063/1.2981063>>.
- [149] C. M. A. Rio and J. Brandao, *Mol. Phys.* **105** (4), 359–373 (2007). <<https://doi.org/10.1080/00268970601161582>>.
- [150] M. H. Alexander, E. J. Rackham, and D. E. Manolopoulos, *J. Chem. Phys.* **121** (11), 5221–5235 (2004). <<https://doi.org/10.1063/1.1779574>>.
- [151] J. Hernando, R. Sayós, and M. González, *Chem. Phys. Lett.* **380** (1), 123–134 (2003). <<https://www.sciencedirect.com/science/article/pii/S0009261403014635>>.
- [152] T. Takayanagi, *J. Chem. Phys.* **116** (6), 2439–2446 (2002).

- <<https://doi.org/10.1063/1.1434988>>.
- [153] T. E. Carroll and E. M. Goldfield, *J. Phys. Chem. A* **105** (11), 2251–2256 (2001). <<https://doi.org/10.1021/jp0037854>>.
- [154] P. Honvault and J. M. Launay, *J. Chem. Phys.* **114** (3), 1057–1059 (2001). <<https://doi.org/10.1063/1.1338973>>.
- [155] A. J. Alexander, F. Javier Aoziz, L. Bañares, M. Brouard, and J. P. Simons, *Phys. Chem. Chem. Phys.* **2**, 571–580 (2000). <<https://doi.org/10.1039/A908928D>>.
- [156] S. K. Gray, C. Petrongolo, K. Drukker, and G. C. Schatz, *J. Phys. Chem. A* **103** (47), 9448–9459 (1999). <<https://doi.org/10.1021/jp991601j>>.
- [157] S. K. Gray, E. M. Goldfield, G. C. Schatz, and G. G. Balint-Kurti, *Phys. Chem. Chem. Phys.* **1** (6), 1141–1148 (1999). <<https://doi.org/10.1039/A809325C>>.
- [158] K. Drukker and G. C. Schatz, *J. Chem. Phys.* **111** (6), 2451–2463 (1999). <<https://doi.org/10.1063/1.479522>>.
- [159] F. Aoziz, L. Bañares, J. Castillo, M. Brouard, W. Denzer, C. Vallance, P. Honvault, J. Launay, A. Dobbyn, and P. Knowles, *Phys. Rev. Lett.* **86** (9), 1729–1732 (2001). <<https://doi.org/10.1103/PHYSREVLETT.86.1729>>.
- [160] K. Yuan, Y. Cheng, X. Liu, S. Harich, X. Yang, and D. H. Zhang, *Phys. Rev. Lett.* **96**, 103202 (2006). <<https://link.aps.org/doi/10.1103/PhysRevLett.96.103202>>.
- [161] F. J. Aoziz, L. Bañares, J. F. Castillo, V. J. Herrero, and B. Martínez-Haya, *Phys. Chem. Chem. Phys.* **4**, 4379–4385 (2002). <<http://dx.doi.org/10.1039/B203755F>>.
- [162] R. K. Talukdar and A. Ravishankara, *Chem. Phys. Lett.* **253** (1), 177 – 183 (1996). <<http://www.sciencedirect.com/science/article/pii/0009261496002035>>.
- [163] R. F. Heidner III and D. Husain, *Inter. J. Chem. Kinet.* **5** (5), 819–831 (1973). <<https://onlinelibrary.wiley.com/doi/abs/10.1002/kin.550050509>>.
- [164] Z. Sun, S. Y. Lin, and Y. Zheng, *J. Chem. Phys.* **135** (23), 234301 (2011). <<https://doi.org/10.1063/1.3668084>>.
- [165] G. B. Pradhan, N. Balakrishnan, and B. K. Kendrick, *J. Phys. B: At. Mol. Opt. Phys.* **47** (13), 135202 (2014). <<https://doi.org/10.1088/0953-4075/47/13/135202>>.
- [166] S. Koppe, T. Laurent, P. Naik, H. R. Volpp, J. Wolfrum, T. Arusi-Parpar, I. Bar, and S. Rosenwaks, *Chem. Phys. Lett.* **214** (6), 546–552 (1993). <<https://www.sciencedirect.com/science/article/pii/000926149385681D>>.
- [167] A. S. Zyubin, A. M. Mebel, S. Der Chao, and R. T. Skodje, *J. Chem. Phys.* **114** (1), 320–330 (2001). <<https://doi.org/10.1063/1.1329887>>.
- [168] T. S. Ho, T. Hollebeek, H. Rabitz, S. Der Chao, R. T. Skodje, A. S. Zyubin, and A. M. Mebel, *J. Chem. Phys.* **116** (10), 4124–4134 (2002). <<https://doi.org/10.1063/1.1431280>>.
- [169] B. Maiti, G. C. Schatz, and G. Lendvay, *J. Phys. Chem. A* **108** (41), 8772–8781 (2004). <<https://doi.org/10.1021/jp049143o>>.
- [170] S. H. Lee and K. Liu, *Chem. Phys. Lett.* **290** (4), 323 – 328 (1998). <[https://doi.org/10.1016/S0009-2614\(98\)00535-1](https://doi.org/10.1016/S0009-2614(98)00535-1)>.
- [171] S. H. Lee and K. Liu, *J. Phys. Chem. A* **102** (45), 8637–8640 (1998). <<http://doi.org/10.1021/jp983220w>>.
- [172] Y. Inagaki, S. M. Shamsuddin, Y. Matsumi, and M. Kawasaki, *Laser Chem.* **14**, 235–244 (1994). <<http://dx.doi.org/10.1155/1994/86820>>.
- [173] S. D. Chao and R. T. Skodje, *J. Phys. Chem. A* **105** (11), 2474–2484 (2001). <<https://doi.org/10.1021/jp003184c>>.
- [174] L. Bañares, J. F. Castillo, P. Honvault, and J. M. Launay, *Phys. Chem. Chem. Phys.* **7**, 627–634 (2005). <<https://doi.org/10.1039/B417368F>>.
- [175] M. Lara, F. Dayou, and J. M. Launay, *Phys. Chem. Chem. Phys.* **13**, 8359 (2011). <<https://doi.org/10.1039/c0cp02091e>>.
- [176] M. Lara, S. Chefdeville, P. Larrégaray, L. Bonnet, J. M. Launay, M. Costes, C. Naulin, and A. Bergeat, *J. Phys. Chem. A* **120** (27), 5274–5281 (2016). <<https://doi.org/10.1021/acs.jpca.6b01182>>.
- [177] M. Lara, S. Chefdeville, K. M. Hickson, A. Bergeat, C. Naulin, J. M. Launay, and M. Costes, *Phys. Rev. Lett.* **109**, 133201 (2012). <<https://doi.org/10.1103/PhysRevLett.109.133201>>.

- [178] D. Dey and A. K. Tiwari, *Eur. Phys. J. D* **68** (6), 169 (2014). <<https://10.1140/epjd/e2014-50115-6>>.
- [179] M. Hankel, S. C. Smith, and A. J. C. Varandas, *Phys. Chem. Chem. Phys.* **13**, 13645–13655 (2011). <<https://doi.org/10.1039/C1CP20127A>>.
- [180] M. Hankel, S. C. Smith, and A. J. C. Varandas, *Phys. Scr.* **84** (2), 028102 (2011). <<https://10.1088/0031-8949/84/02/028102>>.
- [181] J. Yuan, D. He, and M. Chen, *Sci. Rep.* **5**, 14594 (2015). <<https://10.1038/srep14594>>.
- [182] N. Bulut, F. Gogtas, and S. Akpınar, *Chem. Phys.* **309** (2), 231 – 237 (2005). <<https://doi.org/10.1016/j.chemphys.2004.09.014>>.
- [183] H. Yang, K. L. Han, G. C. Schatz, S. C. Smith, and M. Hankel, *J. Phys.: Conf. Series* **185**, 012056 (2009). <<https://doi.org/10.1088/1742-6596/185/1/012056>>.
- [184] H. Yang, K. Han, G. C. Schatz, S. C. Smith, and M. Hankel, *Phys. Chem. Chem. Phys.* **12**, 12711–12718 (2010). <<https://doi.org/10.1039/C0CP00850H>>.
- [185] Y. Z. Song and A. J. C. Varandas, *J. Chem. Phys.* **130** (13), 134317 (2009). <<https://doi.org/10.1063/1.3103268>>.
- [186] Y. Z. Song, P. J. S. B. Caridade, and A. J. C. Varandas, *J. Phys. Chem. A* **113** (32), 9213–9219 (2009). <<https://doi.org/10.1021/jp903790h>>.
- [187] P. Honvault and J. M. Launay, *Chem. Phys. Lett.* **370** (3), 371 – 375 (2003). <[https://doi.org/10.1016/S0009-2614\(03\)00132-5](https://doi.org/10.1016/S0009-2614(03)00132-5)>.
- [188] L. Bañares, F. J. Aoiz, P. Honvault, and J. M. Launay, *J. Phys. Chem. A* **108** (9), 1616–1628 (2004). <<https://doi.org/10.1021/jp037109o>>.
- [189] M. Lara, P. G. Jambrina, A. J. C. Varandas, J. M. Launay, and F. J. Aoiz, *J. Chem. Phys.* **135** (13), 134313 (2011). <<https://doi.org/10.1063/1.3644337>>.
- [190] M. Lara, F. Dayou, J. M. Launay, A. Bergeat, , K. M. Hickson, C. Naulin, and M. Costes, *Phys. Chem. Chem. Phys.* **13**, 8127–8130 (2011). <<https://doi.org/10.1039/c0cp02705g>>.
- [191] L. Bonnet, P. Larrégaray, M. Lara, and J. M. Launay, *J. Phys. Chem. A* **123** (30), 6439–6454 (2019). <<https://doi.org/10.1021/acs.jpca.9b04938>>.
- [192] P. G. Jambrina, M. Lara, M. Menéndez, J. M. Launay, and F. J. Aoiz, *J. Chem. Phys.* **137** (16), 164314 (2012). <<https://doi.org/10.1063/1.4761894>>.
- [193] A. Chang and S. Lin, *Chem. Phys. Lett.* **320** (1), 161 – 168 (2000). <[https://doi.org/10.1016/S0009-2614\(00\)00226-8](https://doi.org/10.1016/S0009-2614(00)00226-8)>.
- [194] A. Khachatrian and P. J. Dagdigian, *J. Chem. Phys.* **122** (2), 024303 (2005). <<https://doi.org/10.1063/1.1827598>>.
- [195] J. A. Klos, P. J. Dagdigian, and M. H. Alexander, *J. Chem. Phys.* **127** (15), 154321 (2007). <<https://doi.org/10.1063/1.2790441>>.
- [196] T. P. Grozdanov and R. McCarroll, *J. Phys. Chem. A* **121** (1), 40–44 (2017). <<https://doi.org/10.1021/acs.jpca.6b11449>>.
- [197] K. Schofield, *J. Phys. Chem. Ref. Data* **8** (3), 723–798 (1979). <<https://doi.org/10.1063/1.55560>>.
- [198] P. Fowles, M. deSorgo, A. J. Yarwood, O. P. Strausz, and H. E. Gunning, *J. Amer. Chem. Soc.* **89** (6), 1352–1362 (1967). <<https://doi.org/10.1021/ja00982a013>>.
- [199] G. Black and L. E. Jusinski, *J. Chem. Phys.* **82** (2), 789–793 (1985). <<https://doi.org/10.1063/1.448504>>.
- [200] G. Black, *J. Chem. Phys.* **84** (3), 1345–1348 (1986). <<https://doi.org/10.1063/1.45052>>.